The spatial properties of adaptation-induced distance compression

Ljubica Jovanovic School of Psychology, University of Nottingham, Nottingham, UK ✉

Paul V. McGraw School of Psychology, University of Nottingham, Nottingham, UK ✉

Neil W. Roach School of Psychology, University of Nottingham, Nottingham, UK ✉

Alan Johnston School of Psychology, University of Nottingham, Nottingham, UK ✉

Exposure to a dynamic texture reduces the perceived separation between objects, altering the mapping between physical relations in the environment and their neural representations. Here we investigated the spatial tuning and spatial frame of reference of this aftereffect to understand the stage(s) of processing where adaptation-induced changes occur. In Experiment 1, we measured apparent separation at different positions relative to the adapted area, revealing a strong but tightly tuned compression effect. We next tested the spatial frame of reference of the effect, either by introducing a gaze shift between adaptation and test phase (Experiment 2) or by decoupling the spatial selectivity of adaptation in retinotopic and world-centered coordinates (Experiment 3). Results across the two experiments indicated that both retinotopic and world-centered adaptation effects can occur independently. Spatial attention to the location of the adaptor alone could not account for the world-centered transfer we observed, and retinotopic adaptation did not transfer to world-centered coordinates after a saccade (Experiment 4). Finally, we found that aftereffects in different reference frames have a similar, narrow spatial tuning profile (Experiment 5). Together, our results suggest that the neural representation of local separation resides early in the visual cortex, but it can also be modulated by activity in higher visual areas.

Introduction

Topographical maps are omnipresent in the human cortex (Sereno, Pitzalis, & Martinez, 2001; Silver & Kastner, 2009; Swisher, Halko, Merabet, McMains, & Somers, 2007; Wandell, Dumoulin, & Brewer, 2007; Wandell & Winawer, 2011). The structure of early visual cortex reflects the spatial layout of retinal receptors, preserving the link between the visual directions of locations in external space and the ordering of activity in the spatial map. However, perceived geometric properties of objects and their spatial relations are not determined simply by the layout of the activation they evoke on the retina or cortical surface, and a mechanistic understanding of the transformation of local activation on the retina to the perceived relations between objects is elusive. For example, after exposure to an object, perceived geometrical properties or features of other objects presented at the same location can change, suggesting plasticity of the underlying mechanisms (Blakemore & Sutton, 1969; Köhler & Wallach, 1944; Webster & Maclin, 1999). These robust effects suggest that the spatial arrangement of the retinal or cortical image is not sufficient to explain perceived size or spatial relations of objects in the visual field.

It has been proposed that lateral connections in the visual cortex could mediate plasticity in the perception of spatial location (Gilbert, Das, Ito, Kapadia, & Westheimer, 1996; Song, Haun, & Tononi, 2017). However, the spatial reach of lateral connections across the visual cortex is limited and therefore cannot explain changes in perceived spatial relations extending beyond those limits (Stettler, Das, Bennett, & Gilbert, 2002). Functional magnetic resonance brain imaging studies have reported that the size of the activated area of V1 is related to the perceived rather than retinal size of a stimulus (Murray, Boyaci, & Kersten, 2006; Pooresmaeili, Arrighi, Biagi, &

Morrone, 2013; Sperandio, Chouinard, & Goodale, 2012). The lateral occipital cortex and the superior parietal cortex have also been implicated in illusory size perception (Kreutzer, Weidner, & Fink, 2015; Plewan, Weidner, Eickhoff, & Fink, 2015; Shen, Zhang, & Chen, 2016; Zeng, Fink, & Weidner, 2020), with feedback projections to the early visual areas having been proposed to mediate the changes seen in early visual cortex (Chen et al., 2019; Koivisto, Railo, Revonsuo, Vanni, & Salminen-Vaparanta, 2011; Zeng et al., 2020). Furthermore, there is some evidence that size aftereffects can transfer across space (Altan & Boyaci, 2020; Corbett & Melcher, 2013), suggesting that additional mechanisms beyond primary visual cortex contribute to size perception.

Recently, it has been shown that apparent separation between two dots or the size of an object can be compressed after adaptation to an irregular dynamic lattice (Hisakata, Nishida, & Johnston, 2016). In the work reported here, we used this robust aftereffect to further investigate how spatial relations between objects are determined by testing its spatial reach and frame of reference.

The average size of neurons' receptive fields and the extent of their lateral connections increase across the hierarchy of the visual pathway (Blatt, Andersen, & Stoner, 1990; Cavanaugh, Bair, & Movshon, 2002; Felleman & Van Essen, 1987; Fujita, 2002; Kisvárday, Tóth, Rausch, & Eysel, 1997; Lund, Yoshioka, & Levitt, 1993; Stettler et al., 2002; Van Den Bergh, Zhang, Arckens, & Chino, 2010). In humans, the average population receptive field size measured with functional magnetic resonance imaging systematically increases from smaller than 0.4 degrees in V1, to 1 degree in V3 (Amano, Wandell, & Dumoulin, 2009; Dumoulin & Wandell, 2008) , and increases to 6 degrees in some areas of human MT+ (Amano et al., 2009). Lateral connections show the same tendency (Lund et al., 1993; Stettler et al., 2002). Therefore, investigating whether and to what extent the adaptation effects extend in space beyond the adapted area will provide an indication of the location in the visual system at which the adaptation occurs (Ayhan, Bruno, Nishida, & Johnston, 2009; Knapen, Brascamp, Adams, & Graf, 2009).

Similarly, if the compression induced by the adaptation is local to a retinotopic map, we would expect the effect to occur in an eye-centered reference frame. Aftereffects of exposure to texture density and figural aftereffects have previously been found to be retinotopic (Afraz & Cavanagh, 2009; Afraz & Cavanagh, 2008; Durgin & Proffitt, 1996) . However, there is some evidence that motion can alter the spatial position of an object in world-centered rather than retinal coordinates (Turi & Burr, 2012) and that adaptation to average ensemble size is not spatially localized (Corbett & Melcher, 2013). Although neurons whose activity is modulated by gaze direction are found

as early as in primary visual cortex (Nakamura & Colby, 2002; Morris & Kerkelberg, 2019; Trotter & Celebrini, 1999), remapping from retinotopic to world-centered coordinates is considered a function of areas beyond the primary visual cortex (Avossa et al., 2007; Crespi et al., 2011; Duhamel, Bremmer, BenHamed, & Graf, 1997; Fairhall, Schwarzbach, Lingnau, Van Koningsbruggen, & Melcher, 2017b; Galleti, Battaglini, & Fattori, 1995; Galletti, Battaglini, & Fattori, 1993; Gardner, Merriam, Movshon, & Heeger, 2008; Gottlieb & Snyder, 2010; Merriam, Genovese, & Colby, 2007). In particular, remapping from retinal to world-centered coordinates requires a mechanism that combines retinotopic maps and information about the direction and magnitude of eye movements, and the properties of neurons in the parietal cortex make it a good candidate for the support of this function. Neurons in parietal cortex show receptive field remapping (Nakamura & Colby, 2002) and are organized in multiple, multi- and supramodal maps of visual space (Colby & Goldberg, 1999; Sereno & Huang, 2006; Sereno et al., 2001). Furthermore, activity in macaque lateral intraparietal cortex (LIP) and 7a is modulated by eye movements (Andersen, Bracewell, Barash, Gnadt, & Fogassi, 1990; Galletti et al., 1993). In humans, activity in posterior parietal cortex represents memorized saccade goals in gaze-centered coordinates (Medendorp, Goltz, Vilis, & Crawford, 2003), and parietal lesions in humans impair the ability to execute memory-guided saccades (Duhamel, Goldberg, Fitzgibbon, Sirigu, & Grafman, 1992; Heide & Kompf, 1998). Therefore, evidence of an aftereffect in world-centered coordinates would suggest that areas beyond primary visual cortex are involved in encoding of the perceived separation of objects.

In summary, the spatial characteristics of the aftereffect can help elucidate the neural representation of the perceived separation. Specifically, here we investigated the spatial tuning and spatial frame of reference to test at what level in the visual system hierarchy adaptation alters the perceived separation of objects. Having found evidence for narrow tuning and aftereffects in both retinotopic and world-centered coordinates, we investigated relationships and properties of these aftereffects in different coordinate frames to gain better understanding of processes contributing to the perception of objects' spatial relations.

General methods

Apparatus

Stimuli were presented on a Mitsubishi (Chiyoda City, Tokyo, Japan) CRT monitor with refresh rate of 60 Hz, viewed binocularly from a distance of 70 cm with a spatial resolution of 1,152 × 864 pixels and 1 pixel subtending 1.7 arcmin. To prevent large head

movements, a chinrest was used. Experiments were created using MATLAB R2018 and Psychtoolbox-3 (Brainard, 1997) running on a Windows XP operating system in a dark room. Data were analyzed in the RStudio environment, and the package quickpsy (Linares & López-Moliner, 2016) was used for fitting psychometric curves. Demos of the experimental procedures are available at https://osf.io/j6p5w/.

Participants

In total, 18 observers participated in the five experiments. Performance of six observers was tested in Experiment 1, including two of the authors. Seven participants took part in Experiment 2 (two of the authors and two participants who also participated in Experiment 1), Experiment 3 (including three of the authors and one participant who also participated in Experiment 2), and Experiment 4 (including the first author and two participants who took part in Experiment 3). In Experiment 5, performance of nine participants was tested, including the four authors and three participants who took part in Experiments 2 and 3. All participants except the authors were naive to the purpose of the experiment and gave informed consent. Experiments were approved by the University of Nottingham, School of Psychology ethics committee and adhered to the tenets of the Declaration of Helsinki.

Experiment 1

In Experiment 1, we aimed to test the spatial reach of the adaptation aftereffects, in order to investigate the location in the visual system at which the adaptation occurs.

Methods

Stimuli

The adaptor was a dynamic dot pattern consisting of black and white dots presented on a mid-gray background. The pattern subtended 4 degrees of visual angle, vertically and horizontally. There were 25 dots distributed on a regular grid (5 × 5 dots, radius 0.15 degrees). Dots were presented with small uniform random displacements (up to 0.3 degrees) relative to the regular grid, and the luminance of the dots was randomly assigned (either white or black). The random displacements and the luminance of the dots were updated every 300 ms. This was designed to avoid retinal afterimages.

The test stimuli consisted of two pairs of black dots (radius 0.15 degrees of visual angle). The spatial separation between dots in the *standard* pair was 1 degree, and the separation between the *test* pair varied

from 0.75 to 1.25 times the standard separation, in seven steps, identical for all participants. The orientation of the imaginary line between the two dots was randomly chosen on each trial and was identical for both pairs.

Procedure

Each trial started with a white fixation point presented at the center of the screen and a brief sound (800 Hz, 30 ms). The adaptor was presented for 60 s in the first trial and for 5 s (top-up) in each subsequent trial. The adaptor was presented at 6 degrees eccentricity on the horizontal meridian, to the left or the right of the fixation point. The luminance of the fixation point changed from white to dark gray 300 ms before the end of the adaptation period, to cue the change of the display. After 500 ms, two pairs of dots (the standard and the test) appeared for 100 ms. Participants were asked to report which pair, presented to the left or the right from the fixation point, had a greater spatial separation between them by pressing a key on a standard computer keyboard. They were asked to maintain their gaze at the fixation point during the trial. Eye movements were not monitored.

To test the spatial reach of the adaptation effect, the stimuli were presented at different locations relative to the adapted area (Figure 1). The pairs of dots were centered at different locations on an invisible circle around the fixation point, to keep the eccentricity constant across conditions. There were seven different positions of the standard dot pair: The dots were centered on the adapted area, straddled the upper or lower edge of the adapted area (19 degrees of arc), or were centered at 39 or 58 degrees of arc from the center of the adaptor (corresponding to a vertical distance of 3.8 and 5 degrees between the center of the adapted area and the center of the stimuli pair). The test pair of dots was presented 180 degrees of arc away from the standard pair.

Participants completed 14 blocks (7 positions of the test pair × 2 locations of the adaptor and the baseline condition) of 35 trials (5 repetitions of each test separation). In separate blocks, we measured baseline performance without the adaptation. The stimuli were presented on the horizontal meridian only, and the location of the standard and the test pair was counterbalanced (standard presented to the left or right of the fixation point). Each condition (position of stimuli and adapted side) was presented in separate blocks, and trials with the same position of the standard relative to the adaptor on the left and the right side of fixation were collapsed for the analysis.

Results

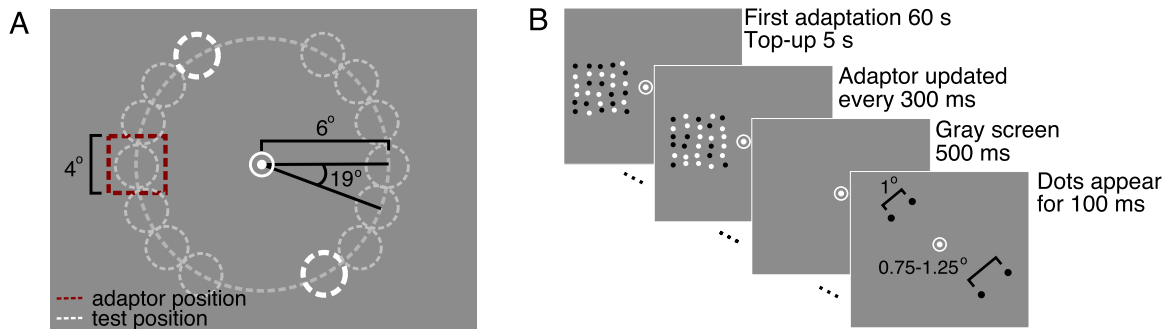We calculated the proportion of responses for which the separation between dots in the test pair

Figure 1. Stimuli layout and sequence in Experiment 1. (A) The adaptor was always presented at an eccentricity of 6 degrees of visual angle on the horizontal meridian, to the left or to the right of the fixation point (in different blocks). To test the spatial tuning of the effect, the standard stimuli pair (constant separation) was presented on the adapted side, at the same location as the adaptor (shown with the red square) or at one of the six other locations, illustrated with gray circles. The test pair was always presented at 180 degrees of arc relative to the standard pair. (B) A trial started with the adaptation phase, during which a lattice of 25 dynamically updating dots was presented. In the first trial of a block, the adaptation phase lasted for 60 s, with 5-s top-ups in subsequent trials. After the adaptation phase, two pairs of black dots were presented on the screen, to the left and right of the fixation point. The participants' task was to report which pair had greater separation between them.

was judged to be greater than that of the standard, as a function of the separation between dots in the test pair, and fitted data with a cumulative normal distribution. We obtained the point of subjective equality (PSE, separation between dots in the test pair judged greater with a probability of 50%) separately for each participant and position of the test relative to the adaptor.

The goodness of fit of the models was assessed by comparing deviances of the models (i.e., the difference between likelihood of the fitted models to those of the saturated models) (e.g., Wichmann & Hill, 2001). We used the bootstrap procedure implemented in the quickpsy package to evaluate the deviance: The parameters of the fit were used to generate 5,000 samples of data, and the deviance of fits on that data was calculated for each bootstrap sample. Using the distribution of bootstrapped deviances, the probability of obtaining a value of deviance greater than that of the original data was calculated, and no significant deviations were detected.

To quantify the adaptation effect, we calculated relative apparent suppression as a ratio between the PSE after adaptation to that of the baseline. Values smaller than 1 indicate compression of the apparent separation following the adaptation. As shown in Figure 2, we found strong compression of the perceived separation between dots when the adaptor and standard stimuli were presented at the same location. The effect of the adaptation was narrowly tuned: It declined when stimuli straddled the adaptor's edge and disappeared when stimuli were presented outside the adapted area. To further quantify these effects, we fitted a Gaussian distribution to the individual PSE as a function of the distance between the adaptor and the test stimuli. This method allowed us to test both whether there are reliable adaptation effects (showing uncertainty as confidence intervals around the fitted curve) and its spatial tuning (the shape or spread of the curve). The average fit across participants is shown in Figure 2 (median R^2 between participants was 0.8, median standard deviation was 13.45 degrees of arc [mad = 3.7]). To obtain a measure of variability associated with the average fit, the data were bootstrapped 5,000 times, and PSEs were obtained for each condition and participant for each bootstrapped sample. We then calculated a median value of each sample across participants to obtain a distribution of the median bootstrapped fit. The dark gray line in Figure 2 indicates the averaged fit, and the shaded area in Figure 2 shows the 95% confidence interval of the distribution of the average (population) fit. This analysis suggests that separation between stimuli presented inside or at the edge of the adapted area (19 degrees of arc) is perceived as compressed, while there is no compression effect further away from the adapted area.

This pattern of results can be predicted by a hypothesis assuming that the strength of the adaptation effect depends on the overlap between the adapted area and the area covered by the standard pair of dots (a circle with a diameter of 1 degree of visual angle). The prediction is shown in open red symbols in Figure 2B.

Experiment 2

In Experiment 1, we found narrow spatial tuning of the adaptation-induced compression of perceived separation, suggesting that the adaptation alters the encoding of spatial distance at early stages of visual processing. To further investigate where in the visual
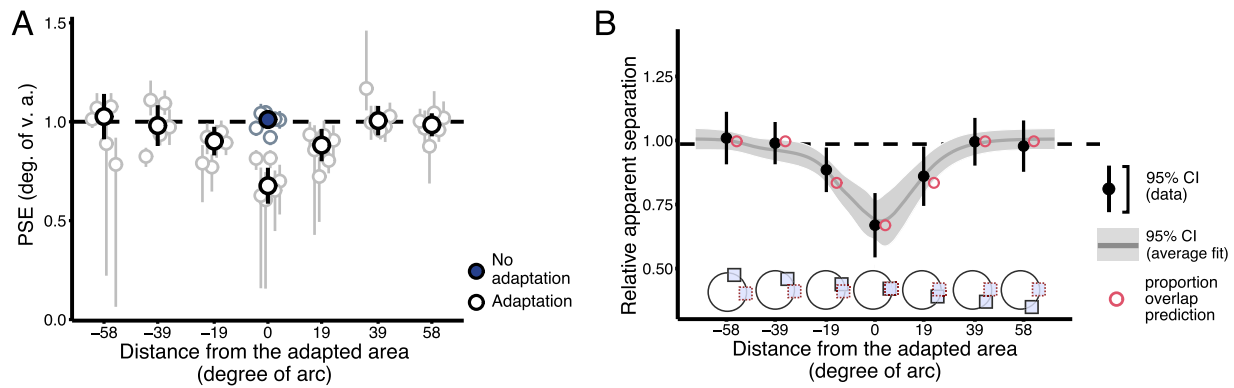
Figure 2. Results of Experiment 1. (A) Individual points of subjective equality for six participants, for the seven positions of the standard relative to the adapted area (open gray symbols), and the control condition (no adaptation, open blue symbols). The error bars on individual data points indicate 95% bootstrapped confidence intervals. The median value across participants is shown with filled symbols, and the corresponding error bars indicate the standard error across participants. (B) The relative apparent separation compression for the seven tested locations. Apparent separation between the standard dots was compressed when the standard was presented at the center of the adapted area, and the effect decreased as the position of the standard pair relative to the adapted area increased. Black symbols show the median across participants. The dark gray line shows the average Gaussian fit calculated across the 5,000 bootstrap samples, and the shaded area indicates the 95% confidence interval obtained by bootstrapping the data. The red symbols indicate predicted values of compression from the degree of overlap between the adapted area and stimuli.

system the adaptation occurs, in Experiment 2, we tested the spatial frame of reference of the adaptation. In particular, we tested whether the aftereffects occur in a retinotopic or world-centered reference frame by introducing a change of gaze direction between the adaptation and test phase.

Methods

Stimuli

The adaptor was similar to that in Experiment 1, with several modifications: The size of the grid was larger (8 × 8 degrees of visual angle), and it consisted of more dots (100, 10 × 10). The color and the dot sizes were the same as in Experiment 1. The spatial separation between the dots in the standard pair was 2 degrees, and the separation between the test pair varied from 0.75 to 1.25 times the standard separation in seven steps.

Procedure

Each trial started with a fixation point presented at 4 degrees of visual angle, to the left or to the right from the center of the screen. The adaptor appeared in the middle of the screen, centered at 4 degrees above or below the horizontal meridian (Figure 3). The adaptor was presented for 60 s in the first trial and 5 s in the rest of the trials of each block. The luminance of the fixation dot decreased 300 ms before the end of the adaptation period, to cue the change of the display. Then, the fixation point changed position twice: first to an intermediate position above or below the adaptor

(depending on where on the screen the adaptor was presented) and then to a final position. The duration between the subsequent changes in position was 800 ms. Participants were asked to follow the changes in the fixation point position with their gaze. Three brief tones (duration: 30 ms; frequency: 800, 1200, and 1600 Hz) were presented at the same time as the fixation point appeared or changed position, to additionally cue the required change of gaze direction. We introduced the intermediate saccade location to match different conditions in terms of eye movements. In the full-adaptation and control conditions, the two saccades were necessary to allow testing the aftereffect with the same gaze direction as in the adaptation phase. To match the number of saccades across the conditions, the intermediate saccade was also introduced in the retinotopic and world-centered conditions.

After the adaptation and eye movement sequences, two pairs of dots appeared and remained on the screen for 100 ms, above or below the screen center. As in the previous experiment, participants were asked to report which pair, presented to the left or the right of fixation, had the greater spatial separation between the two dots. The separation between dots presented in the adapted region was fixed at 2 degrees, and the separation between test dots was varied from 0.75 to 1.25 times the standard separation in seven steps.

There were two adaptor positions, centered on 4 degrees of visual angle, above or below the horizontal meridian. Depending on the position of the adaptor, the intermediate fixation location was either at the top or at the bottom of the screen (8 degrees above or below the center of the screen, at the edge of the adaptor;
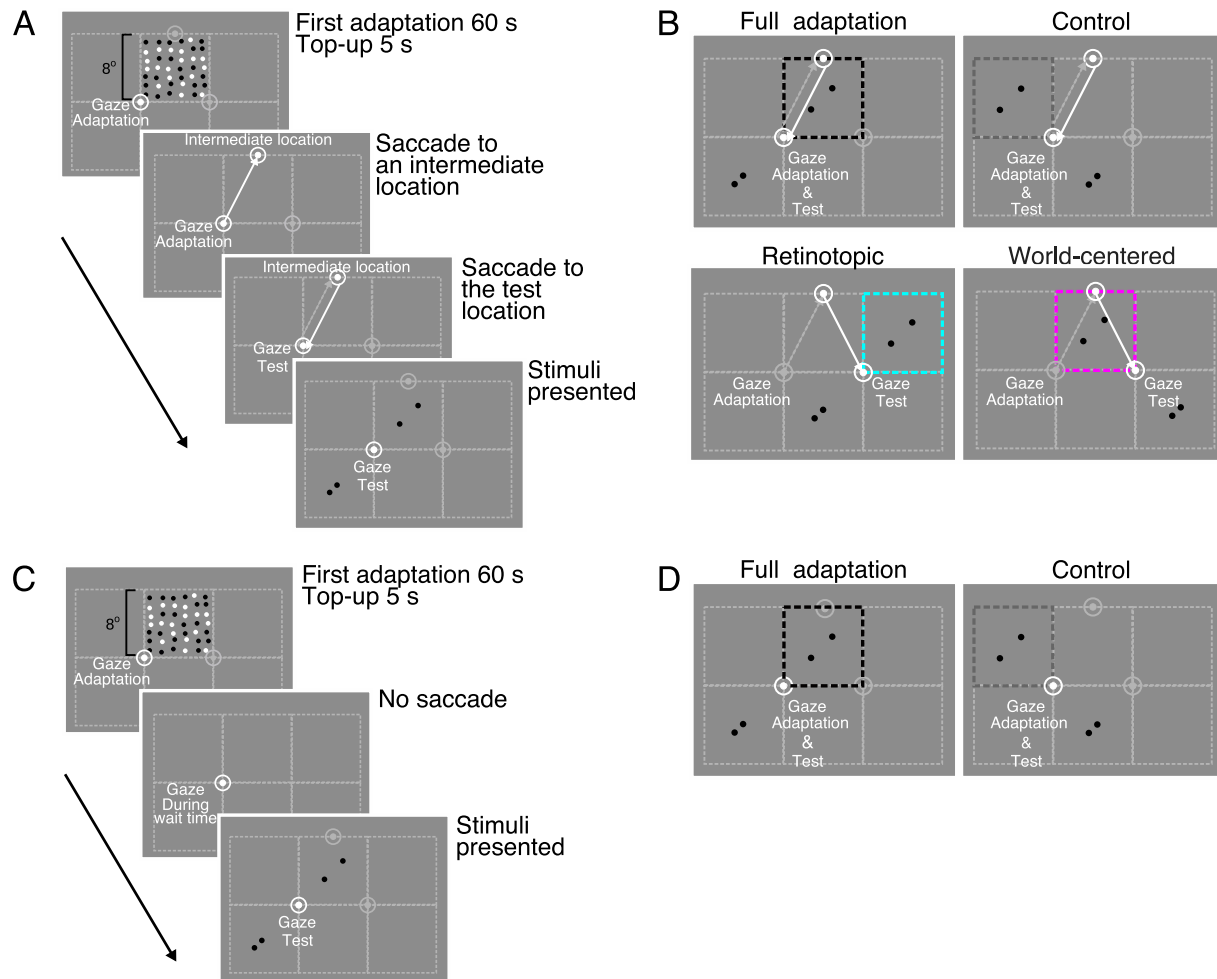
Figure 3. Schematic representation of adaptation procedure and conditions in Experiment 2 in saccade (A, B) and no eye movements (C, D) conditions. (A) During the adaptation phase, the fixation point was presented to the left (shown here) or to the right relative to the center of the screen. The adaptor was presented at the center of the screen, centered at 4 degrees of visual angle above (shown here) or below the horizontal meridian. After the adaptation phase, the fixation point changed location, and participants were asked to follow it with their gaze. After 800 ms, the fixation point changed position again. Then, the standard pair was presented at the adapted or at a control location, and the test pair was presented at the other side of the fixation point. (B) To test performance in the full-adaptation and the control, baseline conditions, in some blocks, the fixation position returned to the same position as during the adaptation phase. Then, the standard pair was presented either at the same location as the adaptor (same retinal and screen coordinates) or on a nonadapted location (shown with black and gray dashed squares, respectively). To test retinotopic and world-centered coordinate frames of adaptation, the fixation point either moved 8 degrees to the right (shown here) or to the left (if its location was on the right side of the screen during the adaptation phase), and participants were asked to execute the second saccade. Then, the standard pair was presented either at the same retinal (magenta square) or screen location (cyan square). (C) To test whether the eye movements have an effect on the apparent separation compression, on some blocks, the fixation point did not change its position after the adaptation phase, and participants were asked to maintain their gaze at the same location throughout the block. Then, the standard stimuli pair was presented either at the adapted location (full adaptation) or at a control, nonadapted location. The temporal interval between the end of adaptation and the test phase was matched to that in the conditions with saccades (1,600 ms). (D) To test performance in the full-adaptation and the control, baseline conditions, in conditions without eye movements, the standard pair was presented either at the same location as the adaptor or at an unadapted location (locations of the standard pair indicated by the black and gray dashed square). As in other conditions, the test pair was always presented at the opposite side of the fixation point relative to the standard pair.
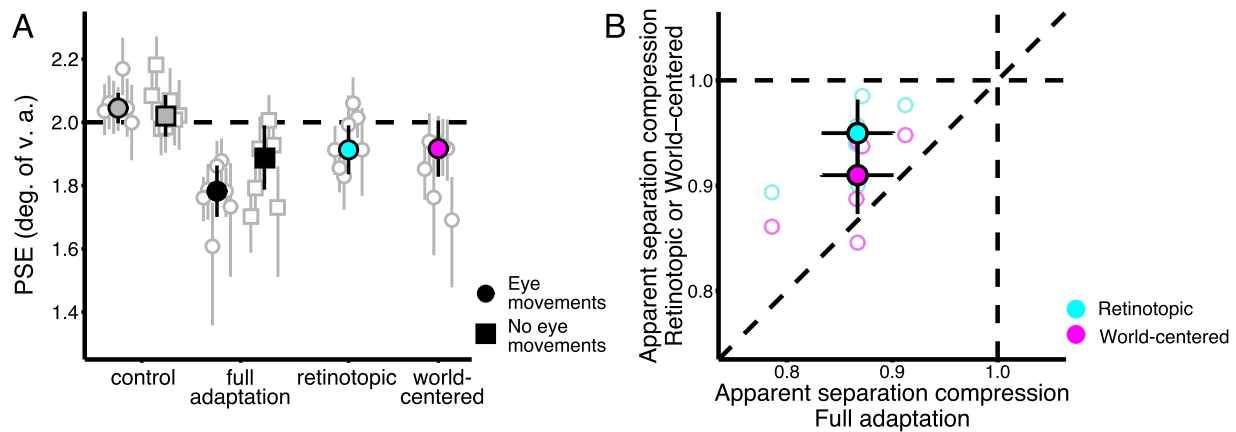
Figure 4. Results of Experiment 2. (A) Point of subjective equality for seven participants, in the four conditions in which participants made eye movements (circles) and two conditions without eye movements (squares). Error bars on individual data points indicate 95% bootstrapped confidence intervals. Median value is shown with filled symbols, and error bars indicate standard error between participants. (B) Relative apparent separation compression in retinotopic (cyan) and world-centered (magenta) conditions plotted against the full-adaptation condition (with eye movements). Perceived separation between the dots presented in the adapted area was smaller than that in the nonadapted region, in each of the three conditions (ratio of PSE in the adaptation condition and the control condition smaller than 1). Open symbols show individual data, and filled symbols show median apparent separation compression for the three conditions. Error bars indicate 95% confidence interval.

Figure 3). In addition, gaze position during fixation was 4 degrees to the left or to the right of the center of the screen. Each condition was tested in a separate block (Figures 3B, D).

We tested six conditions in total. In four conditions, participants were asked to make two eye movements between the adaptation and test phase of the experiment (Figures 3A, B). After fixating an intermediate location, participants directed their gaze either to the same location as during adaptation (upper panels of Figure 3B) or to a different location on the screen 8 degrees away from the first fixation (lower panels of Figure 3B). In the full-adaptation and control conditions, after the intermediate saccade, the fixation position was the same as during the adaptation phase. The standard pair was presented in either an unadapted (control) or an adapted area (full adaptation), to obtain baseline performance and full adaptation–induced compression, respectively. To test whether the adaptation-induced compression occurs in retinotopic or world-centered coordinates, the perceived spatial separation was tested with a different gaze position between the adaptation and test phase of the trial. The standard stimuli pair was presented at either the same retinotopic or the same location on the screen as during adaptation.

To test whether eye movements between the adaptation and the test phase affected distance compression, we also tested performance at the adapted and control locations without the intermediate eye movement (only control and full-adaptation conditions). In these conditions, the temporal interval

between the adaptation and test phase was the same as in the eye movement conditions (Figures 3C, D).

Since conditions were blocked, and the sequence of eye movements was identical within a block, participants could easily perform the required eye movement sequence. An eye tracker (Eyelink 1000, SR Research Ltd.; Ottawa, Ontario, Canada) was used to monitor the eye position during the experiment, and rare trials in which participants did not complete the eye movement sequence correctly were discarded (movement initiated before the cue or gaze shift occurred too late—on average, 3% of trials).

Results

For each participant and condition, we calculated the point of subjective equality, summarized in Figure 4A, for the six conditions. As in Experiment 1, we assessed the goodness of fit of the models by comparing deviances of the models by means of the bootstrap procedure, and no significant deviations were detected.

In order to quantify the effect of the adaptation in the three adaptation conditions (full adaptation, retinotopic, and world centered), we calculated relative apparent separation as a ratio between the PSEs in each adaptation condition and that of the control condition. In this experiment, the three aftereffects were divided by the same PSE obtained in the control condition with eye movements (shown in circles in Figure 4). Relative apparent compression in the retinotopic and world-centered conditions against the full-adaptation

condition (for condition with eye movements) is shown in Figure 4B. Note that the median apparent separation shown in cyan and magenta was calculated over individual apparent separation compressions (individual PSEs divided by the performance in the control condition). Relative apparent adaptation effects were significantly smaller than 1 in each condition (Wilcoxon signed-rank test), indicating that there was a significant adaptation effect in each condition. Next, we compared the magnitude of the aftereffects across different conditions. This comparison can help elucidate the relationship between the effects in different spatial coordinates (e.g., Corbett & Melcher, 2013; Turi & Burr, 2012). A Friedman rank-sum test showed an overall difference between groups ($\chi^2(2) = 10.286$, $p < 0.01$). Post hoc comparisons by means of Wilcoxon signed-rank tests showed that there was no evidence for a difference between the effect in the world-centered condition and the full-adaptation condition (medians 0.87 [$SE = 0.017$] and 0.91 [$SE = 0.018$], respectively), nor was there evidence for a difference between the effect in the world-centered and the retinotopic conditions (medians 0.87 [$SE = 0.017$] and 0.95 [$SE = 0.016$], respectively). Finally, the retinotopic effect was smaller than the effect in the full-adaptation condition.

We did not find evidence for a difference between the relative separation compression with and without eye movements (Wilcoxon signed-rank test, $p = 0.156$).

Experiment 3

The results of Experiment 2 suggest that adaptation-based compression of apparent separation occurs in both retinotopic and world-centered coordinates. However, in the method used in Experiment 2 to probe the spatial frame of reference of the effect, the adaptation phase in the retinotopic and world-centered conditions was the same. Therefore, we cannot say whether adaptation accumulates in both the retinotopic and the world-centered coordinate system or selectively in one (e.g., retinotopic) and transfers to the other coordinate system (e.g., world centered). To tackle this question, in Experiment 3, we modified the adaptation procedure to reduce the contribution of adaptation in either retinotopic or world-centered reference frames *during* the adaptation period.

Methods

Stimuli

The adaptor and stimuli were the same as in Experiment 1.

Procedure

Each participant completed three sessions in random order: retinotopic, world centered, and full adaptation (the adaptor and the standard stimulus shared both retinotopic and world-centered coordinates). In each session, the performance was tested in two conditions: adaptation and control.

The adaptation phase in the full-adaptation session was similar to the adaptation phase in Experiment 2. At the beginning of each trial, a fixation point was presented at the center of the screen. An adaptor was presented at one of four possible locations relative to the fixation point location, in different blocks (6 degrees to the left or the right of the fixation, in the upper or lower hemifield; see Figure 5A). The adaptor was presented for 60 s on the first trial of a block and for 10 s on subsequent trials. After the adaptation phase had finished, two pairs of dots were presented for 100 ms. To test the full-adaptation effect, the standard pair was presented in the adapted region, and the test pair was presented in the nonadapted region (Figure 5D, the two positions above the fixation). To assess baseline performance, apparent spatial separation was measured for two nonadapted regions in separate blocks (Figure 5D, the two positions below the fixation).

Each trial in the retinotopic adaptation session started with the fixation point presented at the center of the screen. Then, the fixation point started to slowly oscillate horizontally on the screen at a constant speed of 3 deg/s. The adaptor was yoked to the position of the fixation point, at 6 degrees to the left or to the right of the fixation, above or below the horizontal meridian, thereby adapting a single retinotopic area but multiple world locations. The upper panel of Figure 5B shows the condition in which the adaptor was presented to the left of the fixation, in the upper visual field. In addition, another adaptor was presented in the part of the visual field opposite to that of the yoked adaptor (Figure 5B, the adaptor is shown below the fixation). This adaptor started moving in the opposite direction relative to the fixation point, at twice the speed (6 deg/s), and the direction of movement reversed on reaching the edge of the screen. Thus, this adaptor covered the same area of screen but at twice the rate of the yoked adaptor. We introduced this adaptor in order to balance attention between the two parts of the visual field and to ensure that at each tested location, the adaptor was presented for approximately the same amount of time in world-centered coordinates (i.e., equalizing the world-centered component of the adaptation), while uncoupling the relative positions of the adapters. The speed and initial direction of motion of the second lattice were chosen as a compromise between the purpose of including the second lattice and the experimental setup available. In particular, we wanted the second lattice to cover a similar amount of
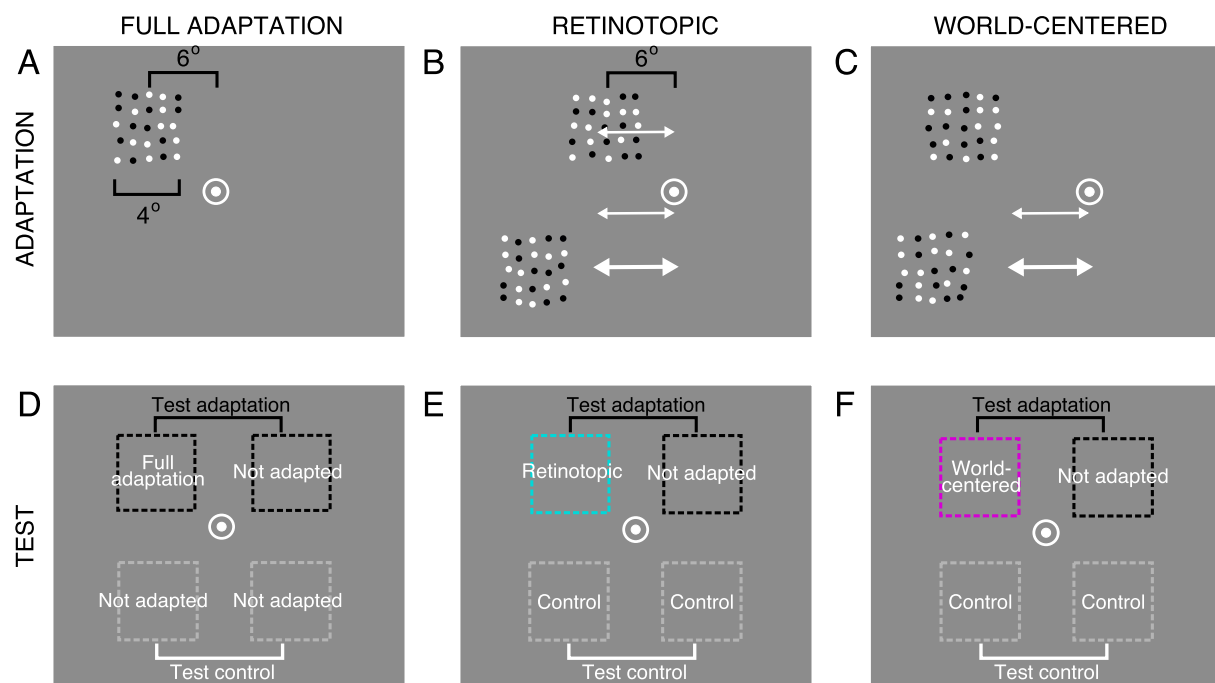
Figure 5. Schematic representation of adaptation phase and conditions in different sessions of Experiment 3; full-adaptation (A, D), retinotopic (B, E), and world-centered (C, F) adaptation sessions. (A) In the full-adaptation session, the fixation point was presented at the center of the screen, and the adaptor was presented 6 degrees to the left (shown here) or to the right, above or below the fixation point. During the adaptation phase, the location of the fixation point and the adaptor remained the same. (B) In the retinotopic adaptation session, at the beginning of each trial, the fixation point was presented at the center of the screen, and the adaptor was presented 6 degrees to the left (shown here) or right, above or below the fixation. During the adaptation phase, the fixation point slowly oscillated across the screen (3 deg/s), and participants were asked to follow it with their gaze. The location of the adaptor was yoked to the position of the fixation point, remaining in the same retinal coordinates during the adaptation phase. A second lattice was presented during the adaptation and started moving across the screen in the opposite direction at twice the speed as the other adaptor and the fixation point. (C) In the world-centered adaptation session, at the beginning of each trial, the fixation point was presented at the center of the screen, and the adaptor was presented 6 degrees to the left (shown here) or right, above or below the fixation. During the adaptation phase, the fixation point slowly oscillated across the screen (3 deg/s), and participants were asked to follow it with their gaze. In this session, the adaptor remained at the same location during the adaptation phase (same screen coordinates). A second lattice was presented during the adaptation and started moving across the screen in the opposite direction at twice the speed as the fixation point. (D) The locations in which adaptation was tested for different conditions in the full adaptation session. To test the control (no adaptation) condition, both the standard and test pair were presented at unadapted locations (shown as white squares). To test the adaptation effect, the standard pair was presented at the adapted location (red square), and the test pair was presented at an unadapted location (black square). (E) The locations in which adaptation was tested in adaptation and control conditions in the retinotopic adaptation session. To test the retinotopic adaptation effect, the standard pair was presented at the adapted location (cyan square), and the test pair was presented at an unadapted location (black square). To test the control condition, both the standard and test pair were presented at the two control locations (here shown below the fixation point with white squares). (F) The locations at which adaptation was tested for the world-centered remapping of adaptation and the control conditions. To test whether the adaptation occurs in screen coordinates, the standard pair was presented at the same location as the adaptor (magenta square), and the test pair was presented at an unadapted location. To test the control condition, both the standard and test pair were presented at the two control conditions locations (here shown below the fixation point).

screen, for a similar amount of time, as the adaptor yoked to the fixation point position and, in the same time, not to adapt a single retinal location. Given the size of the screen, speed of the fixation point, and the location of the adaptor lattice yoked to the position of the fixation point (6 degrees of visual angle), if moving in the opposite direction with the same speed, the

second lattice would reach the border of the screen at a different time to that of the adaptor, whose position was yoked to the position of the fixation point, resulting in the second lattice having a fixed retinal location after the reversal. Therefore, we chose the speed of the second lattice to be twice the speed of the fixation point. The second lattice started moving in the direction
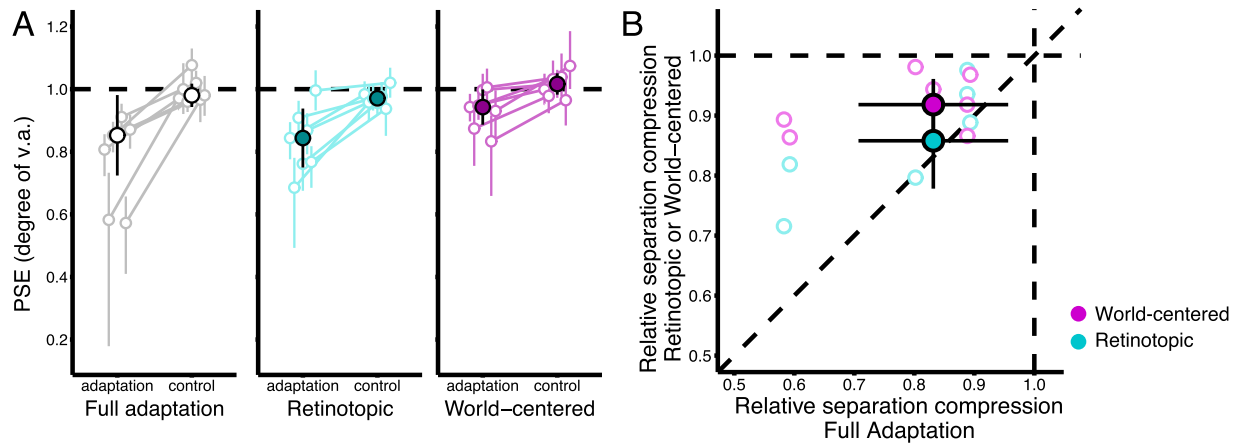
Figure 6. Results of Experiment 3. (A) Points of subjective equality summarized for seven participants, in the three sessions of Experiment 3, for the adaptation and control conditions. Error bars show 95% bootstrapped confidence intervals for each participant and condition. Median values are shown with filled symbols, and corresponding error bars indicate standard error between participants. (B) Relative apparent separation compression in retinotopic and world-centered sessions against the full adaptation session. Open symbols show individual data, and filled symbols show median apparent separation compression for the three sessions. Error bars indicate 95% confidence interval.

opposite to the initial direction of the fixation point, but note that since it was moving at twice the speed, it would reverse its direction sooner than the fixation point, and therefore, for a certain amount of time, the direction of motion of both would be the same. In the first trial of each block, adaptation lasted 60 s, during which the fixation point oscillated along the horizontal meridian (10-s top-ups). The fixation spot changed luminance 300 ms before the end of the adaptation period, to signal the change of the display. To test the degree of adaptation, the standard pair was presented 500 ms after the end of the adaptation period at the adapted retinotopic location, and the comparison pairs were presented either above or below the standard location dependent on the position of the adapter in that block, in the same hemifield (see Figure 5E). This location of the comparison pair corresponded to a retinotopic location that was not adapted during the adaptation phase (since the position of the adaptor was yoked to the oscillating fixation point location). Note that the locations of both the standard and test pairs were equally adapted in the world-centered reference frame. The control condition involved testing at two other locations (see Figure 5E, the two locations below the fixation point) that were equally adapted in both retinotopic and world-centered reference frames. In different blocks, the fixation point began moving either to the right or to the left, and the adaptor was presented at one of the four possible locations relative to fixation and the horizontal meridian (to the left and above or below and, similarly, to the right and above or below).

In the world-centered adaptation session, the adaptation phase was similar to that in the retinotopic session with one important modification. Instead of

moving with the fixation, one of the two adaptors was static on the screen, and therefore a unique area on the screen was being adapted (Figure 5C).

In all conditions, the test pair was presented on the other side of the fixation point relative to the standard pair, and participants estimated which pair had greater separation between the dots. In each condition of each session (adaptation and control), there were 112 trials in total.

An eye tracker was used to monitor the eye position during the experiment, and rare trials in which participants did not follow the fixation point with their gaze sequence correctly were not included in the final analysis (gaze within a 2-degree window relative to the current fixation point location for less than 80% of the trial duration; ∼10% of trials were excluded).

Results

The apparent separation between the standard pair of dots (PSE) is shown in Figure 6A for the six tested conditions. The goodness of fit of the models indicated no significant deviations of the individual fits. We quantified the adaptation in the three adaptation sessions (full adaptation, retinotopic, and world centered) as a ratio between the PSEs in each adaptation condition and that of the control condition, measured separately for each session. Relative apparent compression in retinotopic and world-centered conditions plotted against the full-adaptation condition is shown in Figure 6B. Relative apparent adaptation effects were significantly smaller than 1 in each condition (Wilcoxon test, $p = 0.015$; median [mad]:

full adaptation = 0.83 [0.08], retinotopic 0.86 [0.07], and world centered = 0.92 [0.08]). Friedman rank-sum test did not show a significant difference in apparent compression between conditions ($\chi^2(2) = 4.6$, $p = 0.1$). This pattern of results suggests that aftereffects in both retinotopic and world-centered coordinates can exist independently, implicating at least partly different mechanisms.

Experiment 4

In Experiment 3, we found aftereffects in both retinotopic and world-centered coordinates. To further investigate the nature of the world-centered remapping of the effect and its relation to the retinotopic aftereffect, in Experiment 4, we asked two questions. First, in the conditions in which the world-centered reference frame was tested (Experiments 2 and 3), the adaptor was presented at a single screen location, possibly attracting spatial attention toward it. Previous work has shown that attention to a particular location can alter the appearance of objects (Anton-Erxleben, Henrich, & Treue, 2007; Suzuki & Cavanagh, 1998; Tsal & Shalev, 1996). Here we asked whether a brief adaptor (300 ms), presented just before the saccade, would lead to a separation compression. Second, we also investigated whether retinotopic adaptation can transfer to world-centered coordinates around the time of a saccade. To do this, we measured perceived separation after retinotopic adaptation but included a saccade at the end of the adaptation phase to test whether adaptation transfers to world-centered coordinates. If adaptation at a particular retinal location was remapped to world-centered coordinates after a saccade to retain object feature or position stability under eye movements, then we could expect adaptation effects to be observed at the final screen location of the adaptor after a change in fixation.

Methods

Stimuli

The adaptor and stimuli were the same as in Experiment 3.

Procedure

In the control condition, participants were asked to direct their gaze to the fixation point presented at the center of the screen. After 800 ms, the fixation point changed location, 12 degrees to the left or the right horizontally, and participants were asked to direct their gaze to the new location. A brief sound (30 ms, 1200 Hz) was presented to cue the change of the fixation point position. After 800 ms, two pairs of dots were presented and participants' task was to estimate which pair, above or below the horizontal meridian, had a greater separation between them. The two pairs were presented at 6 degrees to the left or to the right of the screen center, depending on the direction of the saccade (if the saccade was to the left, the stimuli were presented 6 degrees to the left and vice versa).

The spatial cueing condition was similar to the control condition. Each trial started with a fixation point at the center of the screen. Then, an adaptor lattice was briefly presented (300 ms) 6 degrees of visual angle to the left or to the right of the fixation point (Figure 7A). The adaptor was presented at four possible locations, in separate blocks. If in a given block participants made a leftward saccade, the adaptor was presented at 6 degrees to the left of the center of the screen and 6 degrees above or below the horizontal meridian. Conversely, if participants made a rightward saccade, the adaptor was presented 6 degrees to the right from the center of the screen, above or below the horizontal meridian. After the adaptor was presented (800 ms), the fixation point location changed, and participants shifted their gaze. Two pairs of stimuli were presented: A standard pair with a fixed separation was presented at the location previously cued by the adaptor and a test pair, presented above or below the standard pair.

In the adaptation transfer condition, the adaptation phase was similar to that in the retinotopic transfer session in Experiment 3. The fixation point slowly moved horizontally on the screen (3 deg/s), and one of the two adaptors (the upper one in Figure 7B) was yoked to the location of the fixation point. The other adaptor started moving in the opposite direction, at twice the speed (6 deg/s). The adaptation phase lasted 55.6 s in the first trial of a block and 18.5 s in each subsequent trial. These values of adaptation duration were chosen so that in each trial, the fixation point crossed the screen twice, and the start and end of the movement were at the center of the screen. As in Experiment 3, the upper and lower part of the visual field were both adapted in world-centered coordinates, in addition to retinotopic adaptation in the area covered by the adaptor, whose location was yoked to the position of the fixation point. After the adaptation phase, the fixation point moved to the left or to the right side of the screen, as in the two other conditions of Experiment 4, and performance in the separation judgment task was tested. The standard pair of dots was presented at the final location of the adaptor yoked to the fixation point position, and the test pair was presented below or above the standard pair, relative to the horizontal meridian.

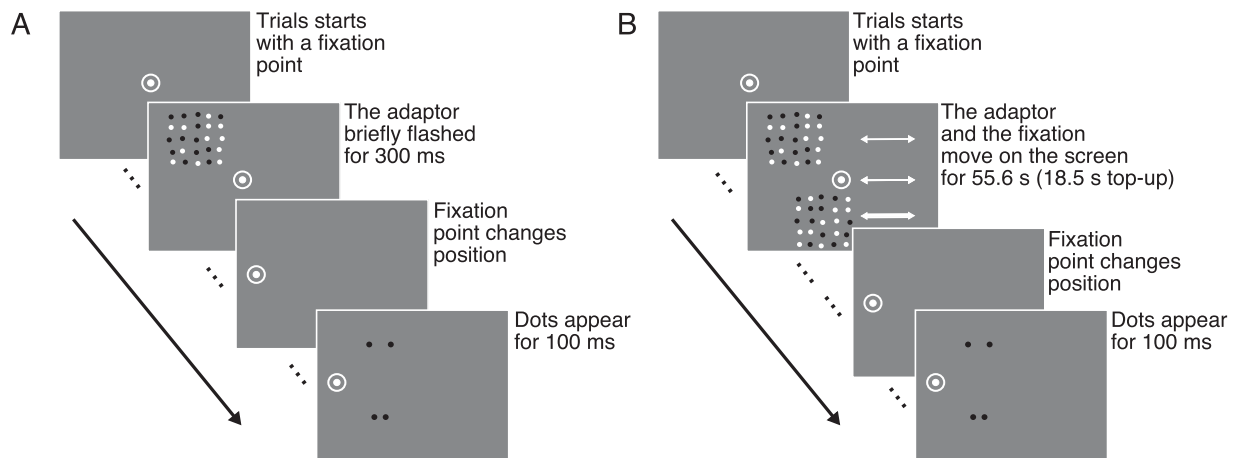In all conditions of Experiment 4, the eye tracker was used to verify that participants correctly executed eye movements.

Figure 7. Schematic representation of the experimental procedure in Experiment 4 in the spatial cueing (A) and adaptation transfer (B) conditions. (A) In the spatial cueing condition, each trial started with a fixation point presentation at the center of the screen. Then, the lattice was briefly (300 ms) presented to the left (shown here) or to the right of the fixation point. After the lattice disappeared, the fixation point changed its position, to the left (shown here) or to the right, depending on where the lattice was presented, and observers were asked to make a saccade to the new location. After 800 ms, two pairs of dots were presented, above and below the horizontal meridian. The standard pair was presented at the same location as the lattice (cued location). (B) In the adaptation transfer condition, each trial started with a fixation point that slowly moved on the screen. Observers were asked to follow its position with their gaze. During the adaptation phase, two adaptors were presented. One was yoked to the position of the fixation point, adapting a single retinal and multiple screen locations. The other adaptor started moving at twice the speed in the opposite direction to that of the fixation point. The adaptation phase finished with the fixation point stopping at the center of the screen. Then, the fixation point changed position to the left or to the right of the center of the screen, and observers were asked to make a saccade to the new location. Following this, two pairs of dots were presented, the standard pair with a fixed separation across trials was presented at the final location of the adaptor whose position was fixed relative to the fixation point (thus at the adaptor's screen location just before the saccade).

Results

As in previous experiments, to quantify the performance, we calculated the PSE for each condition and participant and quantified the compression effects by dividing individual PSEs in the two test conditions by the performance in the control condition. Individual performance and median effects are shown in Figure 8. One participant's eye-tracking data showed that they did not successfully track the slowly oscillating fixation point (more than 2 degrees of visual angle from the center of the fixation, for more than 80% of a trial), and their data for that condition were excluded from the analyses. Wilcoxon signed-rank test showed there was no evidence for separation compression, neither in the adaptation transfer condition (median [mad] = 0.98 [0.025]) nor in the spatial cueing condition (0.95 [0.07]).

In Experiment 4, we found no evidence for effects of spatial cueing on separation compression: When an adaptor was presented for 300 ms before a saccade, no separation compression at the adaptor's location was observed. This finding indicates that the observed world-centered adaptation aftereffect was not a consequence of spatial attention directed to the

adaptor's location. Furthermore, we also asked whether there was a perisaccadic remapping of the aftereffect from the retinotopic to world-centered coordinates. We found no evidence for transfer of adaptation from retinotopic to world-centered coordinates around the time of a saccade. These results suggest that longer exposure of an adaptor at a single screen location is necessary for the world-centered aftereffect and argue against the perisaccadic transfer of adaptation from retinal to world-centered coordinates.

Experiment 5

We found that adaptation-induced compression of apparent separation between dots is encoded in both retinotopic and world-centered coordinates. It has been hypothesized that at least for certain phenomena, aftereffects found in the world-centered coordinate frame could be related to a nonspecific, global spread of adaptation from adapted locations (Corbett & Melcher, 2013; Knapen, Rolfs, Wexler, & Cavanagh, 2010; Mathot & Theeuwes, 2013) . In Experiment 5,
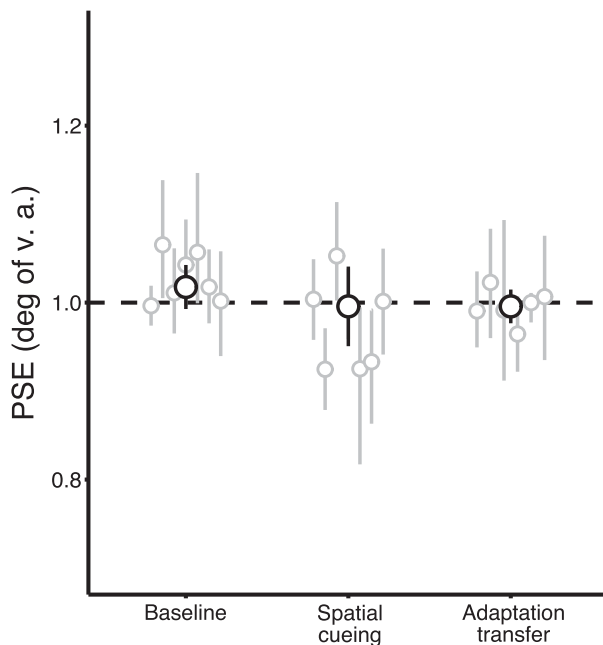
Figure 8. Results of Experiment 4. PSE in the baseline, spatial cueing, and adaptation transfer conditions. Open gray symbols show individual performance and corresponding error bars individual 95% bootstrapped confidence intervals ($N = 5,000$). Open black symbols indicate median PSE, and error bars correspond to 95% confidence interval between participants. There was no evidence for difference between the tested conditions.

we investigated the spatial specificity of the retinotopic and world-centered adaptation effects by testing the apparent separation compression at both adapted and unadapted locations.

Methods

Stimuli

Adaptor and stimuli were the same as in Experiment 3. For one participant, standard separation of dots was increased to 2.5 degrees.

Procedure

The procedure was similar to that of the Experiment 2, with several modifications. Each trial started with a fixation point presented at 4.6 degrees of visual angle relative to the center of the screen, to the left or to the right from the center. The adaptor appeared in the middle of the screen, centered at 3.85 degrees above or below the horizontal meridian (Figure 10). The adaptation phase lasted for 60 s in the first trial and 5 s in the rest of the trials. To test retinotopic and world-centered adaptation aftereffects, in some blocks,

the fixation point changed position after the adaptation phase, and participants were asked to follow changes of the position of the fixation point with their gaze. If in a given block, during the adaptation phase gaze was to the left relative to the center of the screen, the fixation point's position moved 9.2 degrees to the right. Conversely, if the fixation point was presented to the right during the adaptation, the new fixation position was 9.2 degrees of visual angle leftward. Two brief tones (duration: 30 ms; frequency: 800 and 1200 Hz) were presented at the same time as the fixation point appeared or changed position, to additionally cue the required change of gaze direction.

After eye movements were executed, two pairs of dots appeared on the screen for 100 ms, on either side of fixation point. Participants were asked to report which pair had the greater spatial separation between the two dots. Separation between the standard pair (presented at the adapted area) was fixed at 1 degree, and separation between test dots varied between 0.75 and 1.25 times the standard pair. For one participant, the standard separation was increased to 2.5 degrees, since for this participant, after the adaptation, the standard pair of dots appeared too close together to allow enough variability in the responses in order to obtain a psychometric curve. For four participants in some conditions, test spacing was shifted to the 0.5- to 1-degree range, to obtain enough variability to be able to fit data to psychometric curves.

There were two adaptor positions tested in different blocks, centered at 3.85 degrees of visual angle, above or below the horizontal meridian. We tested eight conditions in total. There were four spatial frame of reference conditions: the control condition (baseline), full adaptation, retinotopic, and the world-centered coordinates condition. To test the spatial specificity of each condition, we tested the adaptation effect for standard stimuli presented at the adapted location, or 40 degrees of arc either clockwise or anticlockwise from the adapted location along a notional isoeccentric arc (radius 6 degrees of visual angle). For simplicity, we will refer to these clockwise and anticlockwise positions as "below" and "above" the adapted region, respectively. Note that "adapted location" refers to different locations on the screen and/or retina, depending on the condition. In the full-adaptation condition, the standard was presented at the same retinal and screen coordinates; in the retinotopic condition, the standard was presented at the same retinal but different screen coordinates; and in the world-centered condition, the standard was presented at the same screen but different retinal coordinates than the adaptor.

In the full-adaptation and control conditions, there was no change of gaze direction between the adaptation and test phase, and a standard stimuli pair with a fixed separation across trials was presented in the adapted
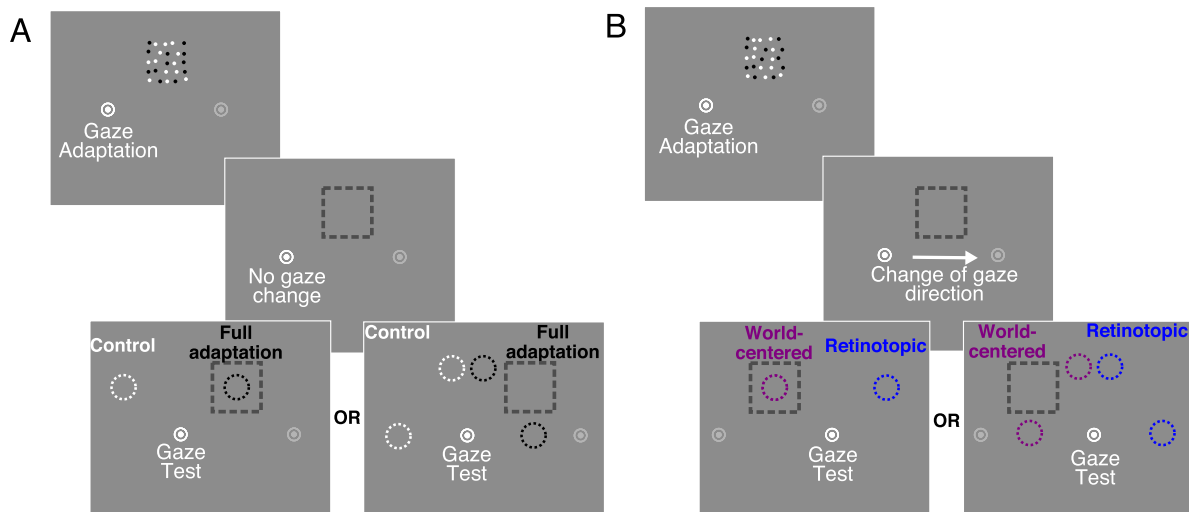
Figure 9. Schematic representation of the experimental procedure in Experiment 5. (A) Procedure in the full-adaptation and control conditions for the two spatial specificity conditions. The adaptor was presented at the center of the screen, at 3.85 degrees of visual angle above (shown here) or below the horizontal meridian. The fixation point was presented 4.6 degrees to the left (shown here) or right from the center of the screen. To test the control (no adaptation) condition and the full adaptation, the fixation point remained at the same location during the test phase. The adapted area is shown as a gray rectangle. Then, a standard stimulus pair (separation 1 degree) was presented either at the same location as the adaptor (full adaptation, shown as a black circle inside the adapted area) or at the other side of the fixation (control, white circle). To test the spatial specificity of the adaptation, in some blocks (shown to the right), the standard was presented above or below the adapted region, at the same eccentricity. (B) Procedure in the retinotopic and world-centered remapping of adaptation conditions for the two spatial specificity conditions. The adaptation phase was the same as in the control and full-adaptation conditions. To test the spatial frame of reference of the adaptation, after the adaptation phase, the fixation point changed position 9.2 degrees to the left or to the right (shown here). To test the world-centered transfer of the adaptation, a standard stimuli pair was presented at the same screen location as the adaptor (purple circle inside the adapted area). To test the retinotopic adaptation, the standard stimulus pair was presented at the same retinotopic location (blue circle). To test the spatial specificity of the remapping of adaptation, in some blocks (shown on the right), the standard was presented above or below the adapted region (relative to the screen or retinotopic coordinates), at the same eccentricity. In all conditions, the test pair was always presented 180 degrees of arc relative to the standard pair, and participants estimated which pair had greater separation between the dots.

or nonadapted control region (Figure 9A, black and white circles, respectively). As in Experiment 2, in the world-centered and retinotopic conditions, the apparent separation was tested with an additional eccentric gaze fixation between the adaptation and the test phase (Figure 9B). The standard pair of dots was presented at either the same retinal or the same screen location as during adaptation (the locations are represented by the blue and purple circles in Figure 9B). To test the spatial specificity of the adaptation, the standard was displaced 40 degrees of arc below or above the center of the adapted area, closely corresponding to one of the tested locations in Experiment 1 (39 degrees of arc). The test pair was always presented at the opposite side of the fixation, and eye movements were monitored to verify that participants executed the eye movements according to task demands. Each condition was tested in a separate block. There were 112 trials in each condition (4 spatial frame of reference conditions × 2 positions relative to the adapted area).

Results

To quantify the performance, we calculated the PSE for each of the eight conditions and each participant. Trials in conditions in which a standard pair was presented below or above the adapted region, as well as the two fixation location conditions (left or right), were grouped together for analysis. We quantified the effects of the adaptation by dividing individual PSEs in the three test conditions by the performance in the control conditions. Individual performance is shown in Figure 10A.

As shown in Figure 10A, B, when stimuli were presented in the adapted area, we found a strong compression of perceived distance in the full-adaptation condition, as indicated by the relative apparent compression smaller than 1 (Wilcoxon signed-rank test $p < 0.05$, Bonferroni corrected, median [mad] = 0.74 [0.06]), and retinotopic condition (Wilcoxon signed-rank test $p < 0.05$, Bonferroni corrected, 0.76 [0.127]).
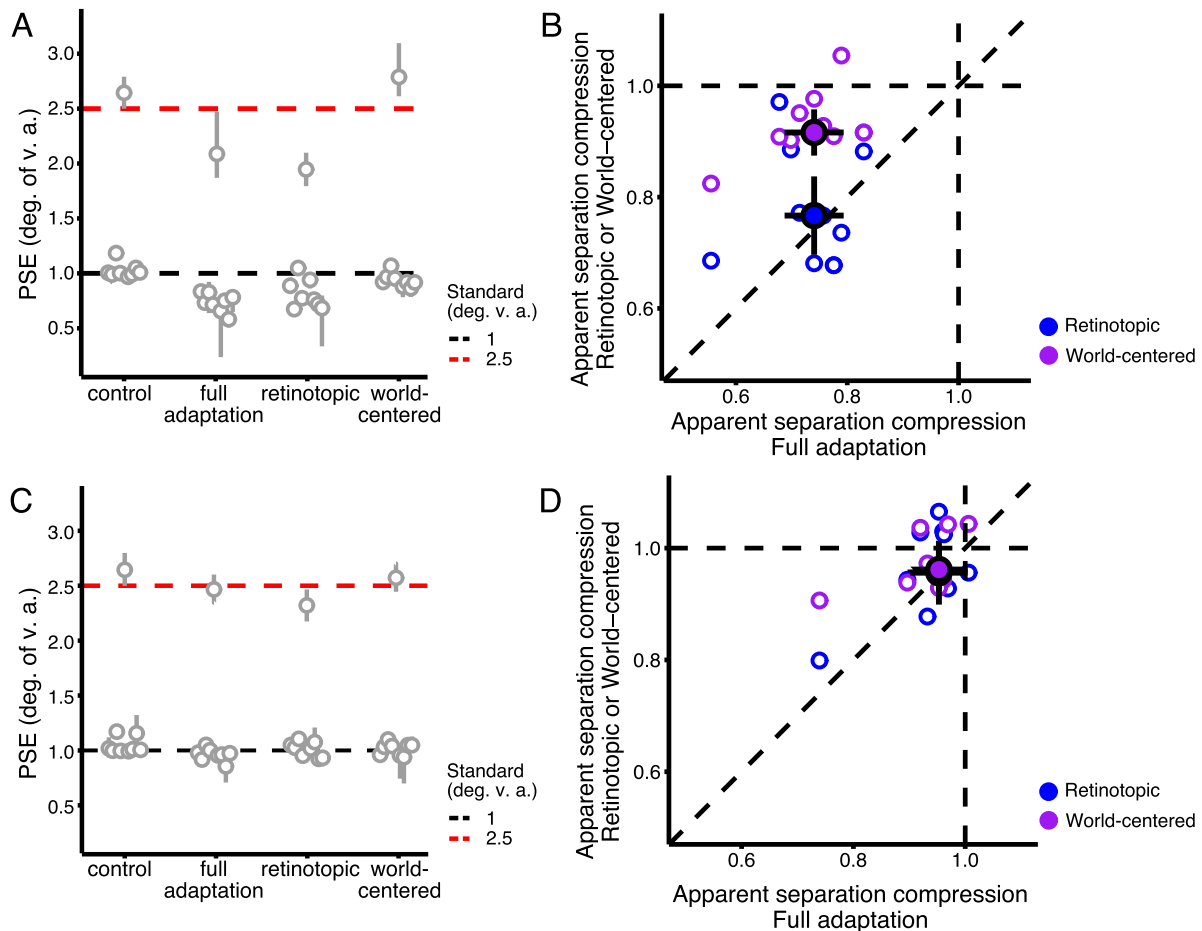
Figure 10. Results of Experiment 5. (A) Point of subjective equality for nine participants in the four conditions, for trials in which the standard stimulus was presented at the adapted location. For one participant, the standard separation was increased to 2.5 degrees (shown in red dashed line). Error bars indicate 95% confidence intervals obtained with bootstrapping the data ($N = 5,000$). (B) Relative apparent separation compression in the retinotopic (dark blue) and world-centered (violet) remapping conditions against the full-adaptation condition, for trials in which standard stimulus was presented at the adapted location. Open symbols show individual data, and filled symbols show median apparent separation compression for the three sessions. Error bars indicate 95% confidence interval over participants. (C) Point of subjective equality for nine participants in the four conditions, for trials in which the standard stimulus was presented above or below the adapted location. For one participant, standard separation was increased to 2.5 degrees (red dashed line). Error bars indicate 95% confidence intervals obtained with bootstrapped data ($N = 5,000$). (D) Relative apparent separation compression in retinotopic (dark blue) and world-centered (violet) remapping conditions against the full-adaptation condition, for trials in which the standard stimulus was presented above or below the adapted location. Open symbols show individual data, and filled symbols show median apparent separation compression for the three sessions. Error bars indicate 95% confidence interval between participants.

We also found a small world-centered effect, which was not significantly different from 1 after correction for multiple comparisons (Wilcoxon signed-rank test $p = 0.117$, Bonferroni corrected, 0.91 [0.019]).

In contrast, in conditions in which spatial spread of adaptation was tested, the relative compression was slightly smaller than 1 only in the full-adaptation condition (Wilcoxon signed-rank test $p = 0.047$, Bonferroni corrected, median [mad] = 0.95 [0.03]). Neither the retinotopic nor world-centered transfer conditions showed significant relative compression (retinotopic: $p = 0.25$, 0.96 [0.11]; world centered: $p = $ 0.2, 0.96 [0.05]). Furthermore, these conditions were not different (Friedman rank-sum test $\chi^2(2) = 1.55$, $p = 0.459$).

Discussion

We investigated the spatial tuning and spatial frame of reference of adaptation-induced apparent separation compression in order to understand at what stage of visual processing these adaptation-induced changes

occur. In Experiment 1, we tested the spatial specificity of the adaptation by asking observers to estimate spatial separation between stimuli at the adapted location or at different distances relative to the adapted area. We found the adaptation-based compression of apparent separation to be narrowly tuned to the location of the adaptor. In Experiment 2, we tested the spatial frame of reference of the adaptation in the classical paradigm: Participants' gaze was directed to a location of a static fixation point during the adaptation phase, and a gaze position change was introduced between the adaptation and test phase. In this experiment, we found evidence that adaptation occurs in both retinotopic and world-centered coordinates. In Experiment 3, we aimed to test whether the adaptation can be found in the two coordinate frames independently. During the adaptation phase, participants pursued with their gaze a slowly moving fixation point. To test the retinotopic component of the adaptation, the adaptor was yoked to the position of the fixation point, adapting a single retinal and multiple screen locations. To test whether the adaptation also occurs at a single screen location, we presented a static adaptor while participants pursued the moving fixation point with their gaze, adapting a single screen and multiple retinal locations. In addition, we tried to minimize allocation of attention to the location of the adaptor by introducing another lattice during the adaptation phase. In both sessions, we found the compression of apparent separation between the dots presented at adapted locations, suggesting that both retinotopic and world-centered adaptation effects on spatial separation can exist independently. In Experiment 4, we tested whether the spatial attention to the location of the adaptor can account for the world-centered transfer we observed, but we did not find evidence to support this hypothesis. Furthermore, we found that retinotopic adaptation did not transfer to world-centered coordinates after a saccade. Finally, in Experiment 5, the spatial spread of adaptation in different coordinate frames was investigated by testing adaptation either at the adapted location or above or below the adapted area. In this experiment, we found a strong spatially confined retinotopic effect but little evidence for significant adaptation in world-centered coordinates.

Evidence for an early site of the apparent distance compression

In Experiment 1, we found a narrow tuning of the effect to the location of the adaptor, suggesting early site of the adaptation in the visual pathway, since both receptive field sizes and horizontal connections scale as a function of the location in the visual processing stream (Amano et al., 2009; Dumoulin & Wandell,

2008; Lund et al., 1993). Average population receptive field size at 6 degrees in human cortical area V1 is estimated to be around 1 degree of visual angle; it is estimated to be 2 degrees in V3 and 8 degrees in TO1 (Amano et al., 2009), localizing the adaptation-induced compression of apparent separation in the early visual cortex. Although we did not record eye movements, fixation instability (e.g., Thaler, Schutz, Goodale, & Gegenfurtner, 2013) could introduce noise during both the adaptation and the test phases, resulting in overestimation of the aftereffect's spatial spread.

Our findings are at odds with a recent study of the size aftereffect (Altan & Boyaci, 2020), in which a very broad tuning was found (up to 8 degrees of visual angle from the adapted area, 10–20% compression, and ~5% expansion of apparent size). However, in this study, eccentricity was confounded with distance between adapted and test locations. Another study found robust compression effects in the absence of any spatial overlap between adaptor and test (Chambers, Johnston, & Roach, 2018). However, in this study, the adaptor was an annulus comprising dots whose luminance was sinusoidally modulated over time, and the test was an array of dipoles (pairs of dots) placed inside the area surrounded by the annular adaptor. Therefore, it is possible that the effect is due to the spatial properties of the adaptor rather than the dynamic dots comprising the annulus, much like in the classical figural aftereffect paradigms (Köhler & Wallach, 1944). Importantly, previous work showed that the adaptation-induced separation compression tested in our study is not equivalent to the size aftereffect: The distance compression induced by a texture adaptation can be found even when size aftereffects are matched between the adapted and nonadapted locations (Hisakata et al., 2016). Therefore, it is possible that unlike the size aftereffects, altered spatial separation processing arising from the dynamic texture adaptor is more narrowly tuned. It should be noted that in Experiment 5, we found a small apparent compression (~5%) in the full-adaptation condition when the standard was presented above or below the adapted area. However, the horizontal and vertical distances from the center of the adapted area were not exactly the same as in Experiment 1, and the procedure was different in order to test the spatial frame of reference of the adaptation. These factors could have contributed to the small discrepancies between the observed tuning in the two experiments.

Across the three experiments, we found a strong and robust retinotopic effect. The effect did not depend on where the adaptor was on the screen during the adaptation phase (Experiments 2 vs. Experiment 3) and did not transfer to world-centered coordinates after a saccade (Experiment 4). Retinotopic aftereffects are considered to have an early origin, since receptive fields have to be small to account for spatially constrained

effects (Gardner et al., 2008). This pattern of results suggests that apparent spatial relations between objects are encoded locally, within retinotopic maps, early in the visual system.

Adaptation aftereffects in world-centered coordinates

In addition to retinotopic effects, we also found evidence for adaptation in world-centered coordinates. It should be noted that although here we use term "world-centered," world(screen)-centered and head-centered coordinates cannot be distinguished in our experiments. We move our eyes frequently, and with each saccade, retinal image changes drastically, but we experience stability of the visual scene. Objects do not change their perceived position in the environment after saccades, suggesting that there must be a fast and efficient mechanism that remaps retinal images to external positions (Durand, Camors, Trotter, & Celebrini, 2012; Fabius, Fracasso, Nijboer, & Van der Stigchel, 2019; Herwig, 2015; Knapen, Swisher, Tong, & Cavanagh, 2016; Rolfs, 2015; Szinte, Jonikaitis, Rolfs, Cavanagh, & Deubel, 2016). Evidence for remapping of adaptation to world-centered coordinates, however, is less clear. Some effects have been disputed or difficult to replicate (Knapen, Rolfs, & Cavanagh, 2009; Knapen et al., 2010; Lescroart, Kanwisher, & Golomb, 2016; Mathot & Theeuwes, 2013; Nishida, Motoyoshi, Andersen, & Shimojo, 2003; Rolfs, 2015). Furthermore, findings interpreted as a consequence of (predictive) remapping are found in locations where they are not expected (Melcher, 2007) and can sometimes be larger than "full-adaptation" effects (Corbett & Melcher, 2013; Turi & Burr, 2012). In Experiment 5, we found a localized adaptation aftereffect in the retinotopic condition but no reliable evidence for aftereffect in the world-centered reference frame. Previous work suggests that world-centered aftereffects can be fragile, for phenomena such as duration compression (Bruno, Ayhan, & Johnston, 2010; Burr, Tozzi, & Morrone, 2007), motion (Knapen, Rolfs, & Cavanagh, 2009; Turi & Burr, 2012), and tilt aftereffects (Knapen, Rolfs, Wexler, & Cavanagh, 2010; Melcher, 2005), although reasons for these inconsistent findings in previous work and this work are not clear. Lack of evidence for an aftereffect in the world-centered reference frame in Experiment 5 is in general agreement with previous work showing that attentional and memory factors can affect the remapping of information about objects in the visual field to world-centered coordinates (Crespi et al., 2011; Laurin et al., 2021; Mathot & Theeuwes, 2011; Prime, Vesia, & Crawford, 2011; Yao, Treue, & Krishna, 2016; Yoshimoto & Takeuchi, 2019). In Experiment 5, in comparison to the earlier experiments, there were

multiple positions on the screen where stimuli were presented across blocks. Although conditions were blocked, blocks were relatively short (∼8 min). These properties of the experimental design could make it more difficult for observers to attend to different locations or keep them in memory, impeding the world-centered adaptation aftereffects.

One suggestion of how visual continuity across saccades is maintained proposes that a signal about a planned saccade is used to update an attentional priority map and facilitate processing at an object's future locations on the retina and in early visual cortex (Cavanagh, Hunt, Afraz, & Rolfs, 2010; Moore, Armstrong, & Fallah, 2003; Wurtz, Joiner, & Berman, 2011). According to this hypothesis, what is being remapped are the spatial locations of targets after saccades, while different features of objects at those locations are processed separately. It has been proposed that visual short-term memories in parietal or frontal areas could store the location of targets, while information about target identity and its features could be encoded in dedicated areas in visual cortices (Ester, Serences, & Awh, 2009; Harrison & Tong, 2009; Medendorp, et al., 2003; Sreenivasan, Curtis, & D'Esposito, 2014).

It is possible that changes in the activity in the local retinotopic maps, induced by shifts in attentional maps while planning the saccade (e.g., LIP, FEF (frontal eye field); Corbetta & Shulman, 2002; Quaia, Optican, & Goldberg, 1998), mimic change in activity in early visual areas induced by adaptation. In particular, attention is known to alter spatial processing at attended locations: spatial frequency is perceived as higher at attended locations, and length is perceived as greater if objects are unattended (Abrams, Barbot, & Carrasco, 2010; Anton-Erxleben et al., 2007; Fang, Boyaci, Kersten, & Murray, 2008; Gobell & Carrasco, 2005; Tsal & Shalev, 1996). We tested this hypothesis in Experiment 4, but found no reliable effect of spatially cueing a location by briefly presenting the adaptor, suggesting that, at least in our paradigm, attention to a spatial location does not lead to effects similar to those observed after the adaptation.

Another interpretation of adaptation aftereffects in a world-centered coordinate frame is feature remapping from retinotopic to world-centered coordinates (Harrison & Tong, 2009; Prime, Niemeier, & Crawford, 2006; Szinte et al., 2016; Zimmermann, Weidner, Abdollahi, & Fink, 2016). Our results are difficult to explain within this context. Results of Experiment 4 suggest no evidence for remapping of retinotopic adaptation to world-centered coordinates around a saccade. Furthermore, we tested adaptation to a dynamic texture on spatial separation of a pair of dots. The adaptor we used had complex temporal and spatial structure, and it is probable that the activity of different filters at several levels of processing was altered after the

adaptation. Finally, the adaptor and test do not share the same features (although the test consisted of the adaptor's elements), and it is not clear which features could be remapped in this case.

Adaptation at different levels in the visual system?

Interestingly, we found that not only can adaptation aftereffects be measured in both retinotopic and world-centered coordinates, but these aftereffects also can exist independently: when only a single retinotopic but multiple-screen coordinates or a single-screen region and multiple retinal locations were being adapted. This finding is consistent with previous work showing that aftereffects can be found in multiple reference frames (Hisakata & Kaneko, 2019; Lauffs, Choung, Ogmen, Herzog, & Kerzel, 2019; Ogmen & Herzog, 2010; Peñaloza, Herzog, & Öğmen, 2020). The finding also suggests that the distance between two objects could depend on different, possibly separate mechanisms: an early representation residing in retinotopic maps and another higher level encoded in world-centered coordinates. Of note, the adaptor we used inevitably had a spatial extent and a shape, and therefore extrastriate visual areas and posterior parietal cortex could also be affected (Chiou & Ralph, 2016; Konen & Kastner, 2008). Consistent with the proposal of separate mechanisms, we found no evidence for transfer of retinotopic adaptation to world-centered coordinates around a saccade. This result does not support the hypothesis that world-centered aftereffects are a consequence of perisaccadic remapping of retinal adaptation (Knapen, Rolfs, & Cavanagh, 2009; Knapen et al., 2010; Lescroart, Kanwisher, & Golomb, 2016; Mathot & Theeuwes, 2013; Nishida et al., 2003; Rolfs, 2015). Activity of higher visual areas such as lateral occipital cortex or posterior parietal cortex was found to be implicated in representations of spatial properties of objects (Larsson & Heeger, 2006; Sayres & Grill-Spector, 2021; Stanley & Rubin, 2003) . Feedback from these areas to striate cortex could mediate the apparent separation compression we observed (Chen et al., 2019; Chen et al., 2021; Dobbins, Jeo, Fiser, & Allman, 1998; Erlikhman & Caplovitz, 2017; Fairhall, Schwarzbach, Lingnau, Van Koningsbruggen, & Melcher, 2017a; Liang et al., 2017; Medendorp, et al., 2003; Silvanto, Lavie, & Walsh, 2005; Sterzer, Haynes, & Rees, 2006; Zeng et al., 2020). Consistent with the feedback hypothesis, there is some evidence that it is the late rather than early activity in early visual cortex relative to the object onset that is correlated with apparent size of objects (Chen et al., 2019; Koivisto et al., 2011; Zeng et al., 2020). For example, TMS (Transcranial Magnetic Stimulation)-induced

disruption of activity in both early visual and lateral occipital cortex changes apparent size perception (Zeng et al., 2020) . The effects of TMS were strongest when it was applied to V1 later than to the lateral occipital cortex, suggesting the importance of feedback to the early visual cortex.

In the aftereffects reported here, dots presented at the same screen location, stimulating same areas on the retina, are perceived as closer in space after exposure to a dynamic texture. It has been proposed that the adaptation changes an internal metric: an explicit neural representation of local scale (Hisakata et al., 2016). Mechanisms transforming local, retinotopic activation evoked by objects in the environment to a sense of spatial relations between those objects is still unknown. In the context of the local metric hypothesis, distance computation can be envisaged as a control process integrating signals corresponding to an elementary unit of the metric. The control process could reside in occipital and parietal areas implicated in the processing of apparent size of objects, such as the lateral occipital cortex or the superior parietal cortex (Kreutzer et al., 2015; Plewan et al., 2015) . Adaptation could reduce the measure of the internal metric, so that activity evoked by the two dots is interpreted as being closer in space. In addition, the control process, originating in higher levels of visual processing, could itself be modified by exposure to the adaptor. Evidence for distinction between the metric and the control process is provided by effects of temporal frequency manipulation of the adapting lattice (Hisakata & Kaneko, 2021). In particular, the spatial separation compression aftereffect was sensitive to frequency of the adaptor update during the adaptation phase, while density aftereffect was not. This dissociation was interpreted as evidence for the metric readout being a distinct mechanism from the local metric (based on density representation), and the magnitude estimation system was proposed as a candidate (Hisakata & Kaneko, 2021; Walsh, 2003). The findings reported here also suggest that the neural representation of local scale resides in early visual cortex, but that apparent separation of objects can also be modulated by activity in higher visual areas. In particular, we found evidence for dual adaptation: The retinotopic and world-centered adaptation aftereffects can exist independently. First, we found retinotopic adaptation aftereffect when no single location in space was adapted, as well as an aftereffect of adaptation of a single screen and multiple retinal coordinates. Furthermore, we found no evidence for transfer of the retinotopic effect to world-centered coordinates after a saccade, providing further evidence for the dissociation.

Acknowledgments

Corresponding author: Ljubica Jovanovic.
Email: lj.m.jovanovic@gmail.com.
Address: School of Psychology, University of Nottingham, Nottingham, UK.

References

Abrams, J., Barbot, A., & Carrasco, M. (2010). Voluntary attention increases. *Attention, Perception & Psychophysics, 72*(6), 1510–1521, https://doi.org/10.3758/APP.

Afraz, A., & Cavanagh, P. (2009). The gender-specific face aftereffect is based in retinotopic not spatiotopic coordinates across several natural image transformations. *Journal of Vision, 9*(10), 1–17, https://doi.org/10.1167/9.10.10.

Afraz, S.-R., & Cavanagh, P. (2008). Retinotopy of the face aftereffect. *Vision Research, 48*, 42–54, https://doi.org/10.1016/j.visres.2007.10.028.

Altan, E., & Boyaci, H. (2020). Size aftereffect is non-local. *Vision Research, 176*, 40–47, https://doi.org/10.1016/j.visres.2020.07.006.

Amano, K., Wandell, B. A., & Dumoulin, S. O. (2009). Visual field maps, population receptive field sizes, and visual field coverage in the human MT+ complex. *Journal of Neurophysiology, 102*, 2704–2718, https://doi.org/10.1152/jn.00102.2009.

Andersen, A., Bracewell, M. R., Barash, S., Gnadt, J. W., & Fogassi, L. (1990). Eye position effects on visual memory, and saccade-related activity in areas LIP and 7a of macaque. *Journal of Neuroscience, 10*(4), 1176–1196.

Anton-Erxleben, K., Henrich, C., & Treue, S. (2007). Attention changes perceived size of moving visual patterns. *Journal of Vision, 7*(11), 1–9, https://doi.org/10.1167/7.11.5.

Avossa, G., Tosetti, M., Crespi, S., Biagi, L., Burr, D. C., & Morrone, M. C. (2007). Spatiotopic selectivity of BOLD responses to visual motion in human area MT. *Nature Neuroscience, 10*(2), 249–255, https://doi.org/10.1038/nn1824.

Ayhan, I., Bruno, A., Nishida, S. Y., & Johnston, A. (2009). The spatial tuning of adaptation-based time compression. *Journal of Vision, 9*(11), 2, https://doi.org/10.1167/9.11.2.

Blakemore, C., & Sutton, P. (1969). Size adaptation: A new aftereffect. *Science, 166*(3902), 245–247.

Blatt, G. J., Andersen, R. A., & Stoner, G. R. (1990). Visual receptive field organization and cortico-cortical connections of the lateral intraparietal area (area LIP) in the macaque. *Journal of Comparative Neurology, 299*, 421–445.

Brainard, D. H. (1997). The Psychophysics Toolbox. *Spatial Vision, 10*(4), 433–436, https://doi.org/10.1163/156856897X00357.

Bruno, A., Ayhan, I., & Johnston, A. (2010). Retinotopic adaptation-based visual duration compression. *Journal of Vision, 10*(10), 30, https://doi.org/10.1167/10.10.30.

Burr, D., Tozzi, A., & Morrone, M. C. (2007). Neural mechanisms for timing visual events are spatially selective in real-world coordinates. *Nature Neuroscience, 10*(4), 423–425.

Cavanagh, P., Hunt, A. R., Afraz, A., & Rolfs, M. (2010). Visual stability based on remapping of attention pointers. *Trends in Cognitive Sciences, 14*(4), 147–153, https://doi.org/10.1016/j.tics.2010.01.007.

Cavanaugh, J. R., Bair, W., & Movshon, A. J. (2002). Nature and interaction of signals from the receptive field center and surround in macaque V1 neurons. *Journal of Neurophysiology, 88*, 2530–2546.

Chambers, A., Johnston, A., & Roach, N. W. (2018). Visual crowding is unaffected by adaptation-induced spatial compression. *Journal of Vision, 18*(3), 1–13, https://doi.org/10.1167/18.3.12.

Chen, J., Sperandio, I., Henry, M. J., Goodale, M. A., Chen, J., Sperandio, I., . . . Goodale, M. A. (2019). Changing the real viewing distance reveals the temporal evolution of size constancy in visual cortex. *Current Biology, 24*, 2237–2243, https://doi.org/10.1016/j.cub.2019.05.069.

Chen, S., Weidner, R., Zeng, H., Fink, G. R., Müller, H. J., & Conci, M. (2021). Feedback from lateral occipital cortex to V1 /V2 triggers object completion: Evidence from functional magnetic resonance imaging and dynamic causal modeling. *Human Brain Mapping, 42*(17), 1–14, https://doi.org/10.1002/hbm.25637.

Chiou, R., & Ralph, M. A. L. (2016). Task-related dynamic division of labor between anterior temporal and lateral occipital cortices in representing object size. *Journal of Neuroscience, 36*(17), 4662–4668, https://doi.org/10.1523/JNEUROSCI.2829-15.2016.

Colby, C. L., & Goldberg, M. E. (1999). Space and attention in parietal cortex. *Annual Review of Neuroscience, 22*, 319–349.

Corbett, J. E., & Melcher, D. (2013). Characterizing ensemble statistics: mean size is represented across multiple frames of reference. *Attention,*

Perception, & Psychophysics, 76(3), 746–758, https://doi.org/10.3758/s13414-013-0595-x.

Corbetta, M., & Shulman, G. L. (2002). Control of goal-directed and stimulus-driven attention in the brain. *Nature Reviews Neuroscience, 3*(3), 201–215.

Crespi, S., Biagi, L., Avossa, G., Burr, D. C., Tosetti, M., & Morrone, M. C. (2011). Spatiotopic coding of BOLD signal in human visual cortex depends on spatial attention. *PLoS ONE, 6*(7), e21661, https://doi.org/10.1371/journal.pone.0021661.

Dobbins, A. C., Jeo, R. M., Fiser, J., & Allman, J. M. (1998). Distance modulation of neural activity in the visual cortex. *Science, 281*, 552–556.

Duhamel, J.-R., Bremmer, F., BenHamed, S., & Graf, W. (1997). Spatial invariance of visual receptive fields in parietal cortex neurons. *Letters to Nature, 389*, 845–848.

Duhamel, J.-R., Goldberg, M. E., Fitzgibbon, E. J., Sirigu, A., & Grafman, J. (1992). Saccadic dysmetrial in a patient with a right frontoparietal lesion. *Brain, 115*, 1387–1402.

Dumoulin, S. O., & Wandell, B. A. (2008). Population receptive field estimates in human visual cortex. *NeuroImage, 39*, 647–660, https://doi.org/10.1016/j.neuroimage.2007.09.034.

Durand, J. B., Camors, D., Trotter, Y., & Celebrini, S. (2012). Privileged visual processing of the straight-ahead direction in humans. *Journal of Vision, 12*(6), 34, https://doi.org/10.1167/12.6.34.

Durgin, F. H., & Proffitt, D. R. (1996). Visual learning in the perception of texture: Simple and contingent aftereffects of texture density. *Spatial Vision, 9*, 423–474, https://doi.org/10.1163/156856896X00204.

Erlikhman, G., & Caplovitz, G. P. (2017). Decoding information about dynamically occluded objects in visual cortex. *NeuroImage, 146*, 778–788, https://doi.org/10.1016/j.neuroimage.2016.09.024.

Ester, E. F., Serences, J. T., & Awh, E. (2009). Spatially global representations in human primary visual cortex during working memory maintenance. *Journal of Neuroscience, 29*(48), 15258–15265.

Fabius, J. H., Fracasso, A., Nijboer, T. C. W., & Van der Stigchel, S. (2019). Time course of spatiotopic updating across saccades. *Proceedings of the National Academy of Sciences, 116*(6), 2027–2203, https://doi.org/10.1073/pnas.1812210116.

Fairhall, S. L., Schwarzbach, J., Lingnau, A., Van Koningsbruggen, M. G., & Melcher, D. (2017a). NeuroImage spatiotopic updating across saccades revealed by spatially-specific fMRI adaptation. *NeuroImage, 147*, 339–345, https://doi.org/10.1016/j.neuroimage.2016.11.071.

Fairhall, S. L., Schwarzbach, J., Lingnau, A., Van Koningsbruggen, M. G., & Melcher, D. (2017b). Spatiotopic updating across saccades revealed by spatially-specific fMRI adaptation. *NeuroImage, 147*, 339–345, https://doi.org/10.1016/j.neuroimage.2016.11.071.

Fang, F., Boyaci, H., Kersten, D., & Murray, S. O. (2008). Attention-dependent representation of a size illusion in human V1. *Current Biology, 18*(21), 1707–1712, https://doi.org/10.1016/j.cub.2008.09.025.

Felleman, D. J., & Van Essen, D. C. (1987). Receptive field properties of neurons in area V3 of macaque monkey extrastriate cortex. *Journal of Neurophysiology, 57*(4), 889–921.

Fujita, I. (2002). The inferior temporal cortex: Architecture, computation, and representation. *Journal of Neurocytology, 31*, 359–371, https://doi.org/10.1023/A.

Galletti, C., Battaglini, P. P., & Fattori, P. (1993). Parietal neurons encoding spatial locations in craniotopic coordinates. *Experimental Brain Research, 96*, 221–229.

Galleti, C., Battaglini, P. P., & Fattori, P. (1995). Eye position influence on the parieto-occipital area PO (V6) of the macaque monkey. *European Journal of Neuroscience, 7*, 2486–2501.

Gardner, J. L., Merriam, E. P., Movshon, A. J., & Heeger, D. J. (2008). Maps of visual space in human occipital cortex are retinotopic, not spatiotopic. *Journal of Neuroscience, 28*(15), 3988–3999, https://doi.org/10.1523/JNEUROSCI.5476-07.2008.

Gilbert, C. D., Das, A., Ito, M., Kapadia, M., & Westheimer, G. (1996). Spatial integration and cortical dynamics. *Proceedings of the National Academy of Sciences, 93*, 615–622.

Gobell, J., & Carrasco, M. (2005). Attention alters the appearance of spatial frequency and gap size. *Psychological Science, 16*(8), 644–651.

Gottlieb, J., & Snyder, L. H. (2010). Spatial and non-spatial functions of the parietal cortex. *Current Opinion in Neurobiology, 20*, 731–740, https://doi.org/10.1016/j.conb.2010.09.015.

Harrison, S. A., & Tong, F. (2009). Decoding reveals the contents of visual working memory in early visual areas. *Nature, 458*, 2–5, https://doi.org/10.1038/nature07832.

Heide, W., & Kompf, D. (1998). Combined deficits of saccades and visuo-spatial orientation after cortical lesions. *Experimental Brain Research, 123*, 164–171.

Herwig, A. (2015). Transsaccadic integration and perceptual continuity. *Journal of Vision, 15*(7), 1–6, https://doi.org/10.1167/15.16.7.doi.

Hisakata, R., Nishida, S., & Johnston, A. (2016). An adaptable metric shapes perceptual space. *Current Biology, 26*, 1911–1915, https://doi.org/10.1016/j.cub.2016.05.047.

Hisakata, R., & Kaneko, H. (2019). Spatial property of the effect of density-adaptation on perceived distances. *Journal of Vision, 19*(8), 55, https://doi.org/10.1167/19.8.55.

Hisakata, R., & Kaneko, H. (2021). Temporal enhancement of cross-adaptation between density and size perception based on the theory of magnitude. *Journal of Vision, 21*(11), 1–11, https://doi.org/10.1167/jov.21.11.11.

Kisvárday, Z. F., Tóth, É., Rausch, M., & Eysel, U. T. (1997). Orientation-specific relationship between populations of excitatory and inhibitory lateral connections in the visual cortex of the cat. *Cerebral Cortex, 7*, 605–618.

Knapen, T., Brascamp, J., Adams, W. J., & Graf, E. W. (2009). The spatial scale of perceptual memory in ambiguous figure perception. *Journal of Vision, 9*(13), 16, https://doi.org/10.1167/9.13.16.

Knapen, T., Rolfs, M., & Cavanagh, P. (2009). The reference frame of the motion aftereffect is retinotopic. *Journal of Vision, 9*(5), 1–6, https://doi.org/10.1167/9.5.16.

Knapen, T., Rolfs, M., Wexler, M., & Cavanagh, P. (2010). The reference frame of the tilt aftereffect. *Journal of Vision, 10*(1), 1–13, https://doi.org/10.1167/10.1.8.

Knapen, T., Swisher, J. D., Tong, F., & Cavanagh, P. (2016). Oculomotor remapping of visual information to foveal retinotopic cortex. *Frontiers in Systems Neuroscience, 10*, 54.

Köhler, W., & Wallach, H. (1944). Figural after-effects: An investigation of visual processes. *American Philosophical Society, 88*(4), 269–357.

Koivisto, M., Railo, H., Revonsuo, A., Vanni, S., & Salminen-Vaparanta, N. (2011). Recurrent processing in V1/V2 contributes to categorization of natural scenes. *Journal of Neuroscience, 31*(7), 2488–2492, https://doi.org/10.1523/JNEUROSCI.3074-10.2011.

Konen, C. S., & Kastner, S. (2008). Two hierarchically organized neural systems for object information in human visual cortex. *Nature Neuroscience, 11*(2), 224–231, https://doi.org/10.1038/nn2036.

Kreutzer, S., Weidner, R., & Fink, G. R. (2015). Rescaling retinal size into perceived size: Evidence for an occipital and parietal bottleneck. *Journal of Cognitive Neuroscience, 27*(7), 1334–1343, https://doi.org/10.1162/jocn.

Larsson, J., & Heeger, D. J. (2006). Two retinotopic visual areas in human lateral occipital cortex.

Journal of Neuroscience, 26(51), 13128–13142, https://doi.org/10.1523/JNEUROSCI.1657-06.2006.

Lauffs, M. M., Choung, O.-H., Ogmen, H., Herzog, M. H., & Kerzel, D. (2019). Reference-frames in vision: Contributions of attentional tracking to nonretinotopic perception in the Ternus-Pikler display. *Journal of Vision, 19*, 1–15, https://doi.org/10.1167/19.12.7.

Laurin, A.-S., Bleau, M., Gedjakouchian, J., Fournet, R., Pisella, L., & Zein Khan, A. (2021). Post-saccadic changes disrupt attended pre-saccadic object. *Journal of Vision, 21*(8), 1–18, https://doi.org/10.1167/jov.21.8.8.

Lescroart, M. D., Kanwisher, N., & Golomb, J. D. (2016). No evidence for automatic remapping of stimulus features or location found with fMRI. *Frontiers in Systems Neuroscience, 10*(53), 1–19, https://doi.org/10.3389/fnsys.2016.00053.

Liang, H., Gong, X., Chen, M., Yan, Y., Li, W., & Gilbert, C. D. (2017). Interactions between feedback and lateral connections in the primary visual cortex. *Proceedings of the National Academy of Sciences, 114*(32), 8637–8642, https://doi.org/10.1073/pnas.1706183114.

Linares, D., & López-Moliner, J. (2016). quickpsy: An R package to fit psychometric functions for multiple groups. *The R Journal, 8*(1), 122–131.

Lund, J. S., Yoshioka, T., & Levitt, J. B. (1993). Comparison of intrinsic connectivity in different areas of macaque monkey cerebral cortex. *Cerebral Cortex, 3*, 148–162.

Mathot, S., & Theeuwes, J. (2011). Visual attention and stability. *Philosophical Transactions of the Royal Society of London. Series B: Biological Sciences, 366*(1564), 516–527, https://doi.org/10.1098/rstb.2010.0187.

Mathot, S., & Theeuwes, J. (2013). A reinvestigation of the reference frame of the tilt-adaptation aftereffect. *Scientific Reports, 3*(1152), 1–7, https://doi.org/10.1038/srep01152.

Medendorp, W. P., Goltz, H. C., Vilis, T., & Crawford, J. D. (2003). Gaze-centered updating of visual space in human parietal cortex. *Journal of Neuroscience, 23*(15), 6209–6214.

Melcher, D. (2005). Spatiotopic transfer of visual-form adaptation across saccadic eye movements. *Current Biology, 15*(19), 1745–1748.

Melcher, D. (2007). Predictive remapping of visual features precedes saccadic eye movements. *Nature Neuroscience, 10*(7), 903–907, https://doi.org/10.1038/nn1917.

Merriam, E. P., Genovese, C. R., & Colby, C. L. (2007). Remapping in human visual cortex.

Journal of Neurophysiology, 97, 1738–1755, https://doi.org/10.1152/jn.00189.2006.

Morris, A. P., & Krekelberg, B. (2019). A stable visual world in primate primary visual cortex. *Current Biology, 29*(9), 1471–1480.

Moore, T., Armstrong, K. M., & Fallah, M. (2003). Visuomotor origins of covert spatial attention. *Neuron, 40*, 671–683.

Murray, S. O., Boyaci, H., & Kersten, D. (2006). The representation of perceived angular size in human primary visual cortex. *Nature Neuroscience, 9*(3), 429–434, https://doi.org/10.1038/nn1641.

Nakamura, K., & Colby, C. L. (2002). Updating of the visual representation in monkey striate and extrastriate cortex during saccades. *Proceedings of the National Academy of Sciences, 99*(6), 4026–4031.

Nishida, S. Y., Motoyoshi, I., Andersen, R. A., & Shimojo, S. (2003). Gaze modulation of visual aftereffects. *Vision Research, 43*(6), 639–649.

Ogmen, H., & Herzog, M. H. (2010). The geometry of visual perception: Retinotopic and nonretinotopic representations in the human visual system. *Proceedings of the IEEE, 98*(3), 479–492.

Peñaloza, B., Herzog, M. H., & Öğmen, H. (2020). Non-retinotopic adaptive center-surround modulation in motion processing. *Vision Research, 174*, 10–21, https://doi.org/10.1016/j.visres.2020.05.007.

Plewan, T., Weidner, R., Eickhoff, S. B., & Fink, G. R. (2015). Ventral and dorsal stream interactions during the perception of the Müller-Lyer illusion: Evidence derived from fMRI and dynamic causal modeling. *Journal of Cognitive Neuroscience, 24*(10), 2015–2029.

Pooresmaeili, A., Arrighi, R., Biagi, L., & Morrone, M. C. (2013). Blood oxygen level-dependent activation of the primary visual cortex predicts size adaptation illusion. *Journal of Neuroscience, 33*(40), 15999–16008, https://doi.org/10.1523/JNEUROSCI.1770-13.2013.

Prime, S. L., Niemeier, M., & Crawford, J. D. (2006). Transsaccadic integration of visual features in a line intersection task. *Experimental Brain Research, 169*, 532–548, https://doi.org/10.1007/s00221-005-0164-1.

Prime, S. L., Vesia, M., & Crawford, D. J. (2011). Cortical mechanisms for trans-saccadic memory and integration of multiple object features. *Philosophical Transactions of the Royal Society B: Biological Sciences, 366*, 540–553, https://doi.org/10.1098/rstb.2010.0184.

Quaia, C., Optican, L. M., & Goldberg, M. E. (1998). The maintenance of spatial accuracy by the perisaccadic remapping of visual receptive fields. *Neural Networks, 11*(7–8), 1229–1240.

Rolfs, M. (2015). Attention in active vision: A perspective on perceptual continuity across saccades. *Perception, 44*(8–9), 900–919, https://doi.org/10.1177/0301006615594965.

Sayres, R., & Grill-Spector, K. (2021). Relating retinotopic and object-selective responses in human lateral occipital cortex. *Journal of Neurophysiology, 100*, 249–267, https://doi.org/10.1152/jn.01383.2007.

Sereno, M. I., & Huang, R.-S. (2006). A human parietal face area contains aligned head-centered visual and tactile maps. *Nature Neuroscience, 9*(10), 1337–1343, https://doi.org/10.1038/nn1777.

Sereno, M. I., Pitzalis, S., & Martinez, A. (2001). Mapping of contralateral space in retinotopic coordinates by a parietal cortical area in humans. *Science, 294*, 1350–1355.

Shen, L., Zhang, M., & Chen, Q. (2016). The Poggendorff illusion driven by real and illusory contour: Behavioral and neural mechanisms. *Neuropsychologia, 85*, 24–34, https://doi.org/10.1016/j.neuropsychologia.2016.03.005.

Silvanto, J., Lavie, N., & Walsh, V. (2005). Double dissociation of V1 and V5/MT activity in visual awareness. *Cerebral Cortex, 15*, 1736–1741, https://doi.org/10.1093/cercor/bhi050.

Silver, M. A., & Kastner, S. (2009). Topographic maps in human frontal and parietal cortex. *Trends in Cognitive Science, 13*(11), 488–495, https://doi.org/10.1016/j.tics.2009.08.005.

Song, C., Haun, A. M., & Tononi, G. (2017). Plasticity in the structure of visual space. *ENeuro, 4*, 1–7.

Sperandio, I., Chouinard, P. A., & Goodale, M. A. (2012). Retinotopic activity in V1 reflects the perceived and not the retinal size of an afterimage. *Nature Neuroscience, 15*(4), 540–543, https://doi.org/10.1038/nn.3069.

Sreenivasan, K. K., Curtis, C. E., & D'Esposito, M. (2014). Revisiting the role of persistent neural activity during working memory. *Trends in Cognitive Sciences, 18*(2), 82–89.

Stanley, D. A., & Rubin, N. (2003). fMRI activation in response to illusory contours and salient regions in the human lateral occipital complex. *Neuron, 37*, 323–331.

Sterzer, P., Haynes, J.-D., & Rees, G. (2006). Primary visual cortex activation on the path of apparent motion is mediated by feedback from hMT + /V5. *NeuroImage, 32*, 1308–1316, https://doi.org/10.1016/j.neuroimage.2006.05.029.

Stettler, D. D., Das, A., Bennett, J., & Gilbert, C. D. (2002). Lateral connectivity and contextual

interactions in macaque primary visual cortex. *Neuron, 36*, 739–750.

Suzuki, S., & Cavanagh, P. (1998). A shape-contrast effect for briefly presented stimuli. *Journal of Experimental Psychology: Human Perception and Performance, 24*(5), 1315–1341.

Swisher, J. D., Halko, M. A., Merabet, L. B., McMains, S. A., & Somers, D. C. (2007). Visual topography of human intraparietal sulcus. *Journal of Neuroscience, 27*(20), 5326–5337, https://doi.org/10.1523/JNEUROSCI.0991-07.2007.

Szinte, M., Jonikaitis, D., Rolfs, M., Cavanagh, P., & Deubel, H. (2016). Presaccadic motion integration between current and future retinotopic locations of attended objects. *Journal of Neurophysiology, 116*(4), 1592–1602, https://doi.org/10.1152/jn.00171.2016.

Thaler, L., Schütz, A. C., Goodale, M. A., & Gegenfurtner, K. R. (2013). What is the best fixation target? The effect of target shape on stability of fixational eye movements. *Vision Research, 76*, 31–42.

Trotter, Y., & Celebrini, S. (1999). Gaze direction controls response gain in primary visual-cortex neurons. *Nature, 398*(6724), 239–242.

Tsal, Y., & Shalev, L. (1996). Inattention magnifies perceived length: The attentional receptive field inattention magnifies perceived length: The attentional receptive field hypothesis. *Journal of Experimental Psychology: Human Perception and Performance, 22*(1), 233–243, https://doi.org/10.1037//0096-1523.22.1.233.

Turi, M., & Burr, D. (2012). Spatiotopic perceptual maps in humans: evidence from motion adaptation. *Proceedings of the Royal Society B: Biological Sciences, 279*, 3091–3097, https://doi.org/10.1098/rspb.2012.0637.

Van Den Bergh, G., Zhang, B., Arckens, L., & Chino, Y. M. (2010). Receptive-field properties of V1 and V2 neurons in mice and macaque monkeys. *Journal of Comparative Neurology, 518*, 2051–2070, https://doi.org/10.1002/cne.22321.

Walsh, V. (2003). A theory of magnitude: Common cortical metrics of time, space and quantity. *Trends in Cognitive Sciences, 7*(11), 483–488.

Wandell, B. A., Dumoulin, S. O., & Brewer, A. A. (2007). Review visual field maps in human cortex. *Neuron, 56*, 366–383, https://doi.org/10.1016/j.neuron.2007.10.012.

Wandell, B. A., & Winawer, J. (2011). Imaging retinotopic maps in the human brain. *Vision Research, 51*(7), 718–737, https://doi.org/10.1016/j.visres.2010.08.004.

Webster, M. A., & Maclin, O. H. (1999). Figural aftereffects in the perception of faces. *Psychonomic Bulletin & Review, 6*(4), 647–653.

Wichmann, F. A., & Hill, N. J. (2001). The psychometric function: I. Fitting, sampling, and goodness of fit. *Perception & Psychophysics, 63*(8), 1293–1313.

Wurtz, R. H., Joiner, W. M., & Berman, R. A. (2011). Neuronal mechanisms for visual stability: Progress and problems. *Philosophical Transactions of the Royal Society B: Biological Sciences, 366*, 492–503, https://doi.org/10.1098/rstb.2010.0186.

Yao, T., Treue, S., & Krishna, S. B. (2016). An attention-sensitive memory trace in macaque MT following saccadic eye movements. *PLoS Biology, 14*(2), 1–17, https://doi.org/10.1371/journal.pbio.1002390.

Yoshimoto, S., & Takeuchi, T. (2019). Effect of spatial attention on spatiotopic visual motion perception. *Journal of Vision, 19*(5), 1–19, https://doi.org/10.1167/19.4.4.

Zeng, H., Fink, G. R., & Weidner, R. (2020). Visual size processing in early visual cortex follows lateral occipital cortex involvement. *Journal of Neuroscience, 40*(22), 4410–4417.

Zimmermann, E., Weidner, R., Abdollahi, R. O., & Fink, G. R. (2016). Spatiotopic adaptation in visual areas. *Journal of Neuroscience, 36*(37), 9526–9534, https://doi.org/10.1523/JNEUROSCI.0052-16.2016.